

## CHAPTER 11: CHEMISTRY/ELECTROCHEMISTRY OF SPENT NUCLEAR FUEL AS A WASTEFORM

David W. Shoesmith,  
Surface Science Western and Department of Chemistry  
Western University,  
London, Ontario, N6A 5B7  
Canada  
e-mail: dwshoesm@uwo.ca

### INTRODUCTION

The direct disposal of spent nuclear fuel in geologic repositories, built several hundred metres underground, has been under consideration internationally for 20 to 30 years. Various geologic formations are being, or have been, studied including tuff rock, salt domes, sedimentary clay deposits and granitic rock. The spent nuclear fuel would be encapsulated and sealed within a metallic container, most likely carbon steel possibly with an outer Cu shell and emplaced in bore holes or deposition tunnels within the repository. The space

between the container and the borehole/tunnel wall would then be backfilled with sealing materials such as clays and clay/sand mixtures. A schematic illustrating the Canadian concept for disposal in crystalline rock is shown in Figure 11-1. This arrangement constitutes a multiple barrier system, Figure 11-2, including the engineered barriers (1, 2, and 3), a geotechnical barrier (4) and the geologic barrier (5). Other national concepts are based on the same multiple barrier concept, but the specific barrier designs may vary (Bennett & Gens 2008).

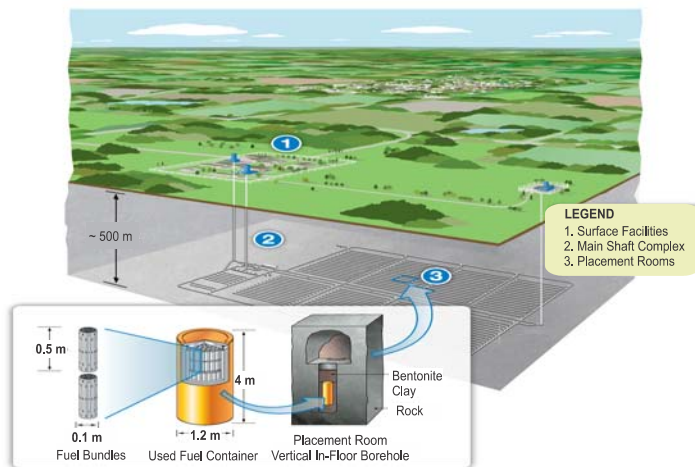
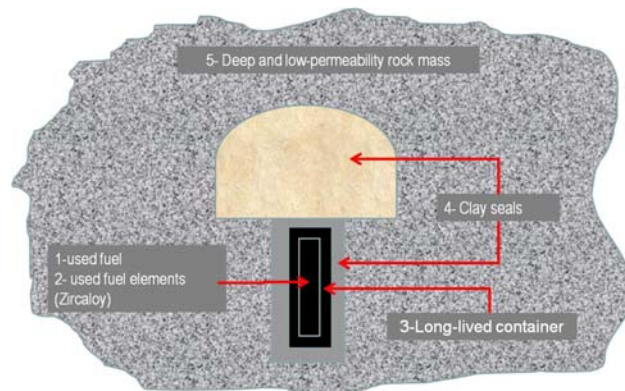


Figure 11-1. Schematic illustration of the Canadian deep geologic repository concept for a crystalline rock location.

Figure 11-2. Schematic illustration of the multi-barrier concept for waste disposal showing the 5 key barriers to radionuclide release and transport



Such a repository can provide reasonable assurance in the long term containment and isolation of the fuel. However, since regulatory radioactivity release limits make it necessary to achieve containment for thousands to tens of thousands of years, an extreme condition by any standard, it is judicious to consider the consequences of container failure leading to exposure of the fuel to groundwater. Since the spent fuel contains the residual radioactivity, its behavior on contact with groundwater provides the critical radioactivity source term in any assessment of repository safety. With this important goal in mind, extensive international studies have been undertaken to understand fuel behavior and predict the rates of radionuclide release.

### DESCRIPTION OF THE FUEL

The universally common form of nuclear fuel is stoichiometric uranium dioxide ( $\text{UO}_{2.001}$ ) fabricated in the form of high density ceramic pellets (94% to 97% of theoretical density). These pellets are generally ~1cm in diameter and length and contained within cladding tubes fabricated from Zircaloy, a corrosion resistant Zr alloy, containing small amounts of Sn, used because of its low neutron capture cross section. The majority of fuel used in light water reactors (LWR) is high purity and enriched (to 1–5%) in the fissile isotope  $^{235}\text{U}$ . By contrast, fuel used in Canadian (CANDU) reactors is unenriched (0.712%  $^{235}\text{U}$ ). Some LWR fuel is mixed oxide (MOX) fuel consisting of  $\text{UO}_2$  blended with up to 5%  $\text{PuO}_2$ . The cladding tubes are sealed by welding and bundled together into either a large LWR assembly 3 to 5 m in length (Fig. 11-3), or a small CANDU fuel bundle (0.5 m in length, Fig. 11-4).

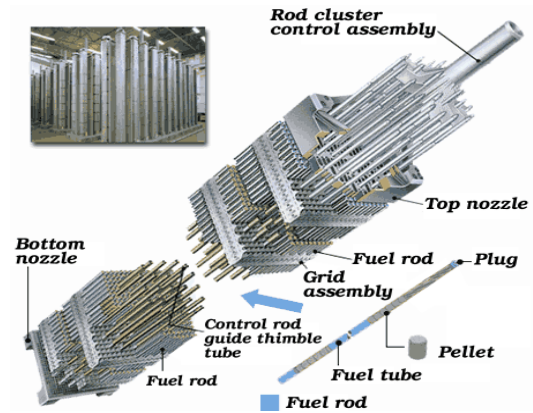
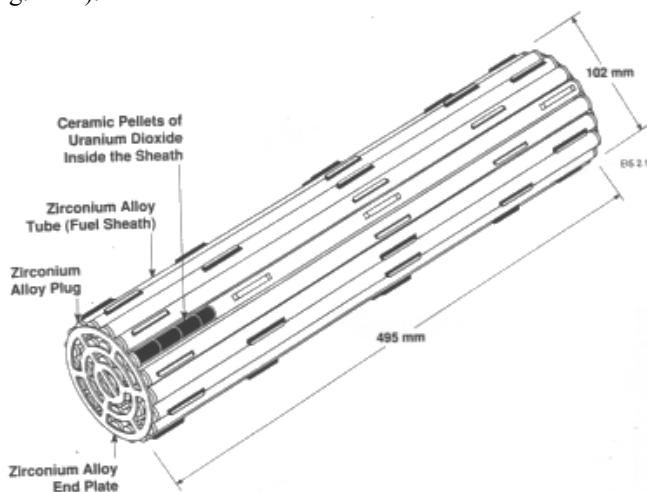
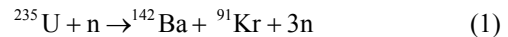


Figure 11-3. Schematic view of a PWR fuel assembly (www.world-nuclear.org).

In-reactor irradiation leads to the formation of a wide range of radionuclides as a result of fission reactions, *e.g.*,



Neutron capture, *e.g.*,



And, to a lesser degree, activation, *e.g.*,



Fission reactions produce heat and LWR fuel can develop a power of 15 to 25 kW/m of fuel during operation, which corresponds to a temperature in the center of the pellet in the range 800 to 1200°C. For CANDU fuel, linear power ratings can be substantially higher leading to center line temperatures up to 1700°C. On discharge from reactor only a few fuel bundles or assemblies have minor damage or defects such as pinholes through the cladding. The nature and number of fuel defects have been recently reviewed (IAEA 2010).

Figure 11-4. Schematic illustration of a Canadian (CANDU) fuel bundle.

Typical burn-ups for LWR fuel are in the range 190 to 960 MWh/kg U (McMurry *et al.* 2003) (120 to 320 MWh/kg U for CANDU fuel, Tait *et al.* 2000) although, more recently, burn-up has been increasing. Burn-up is a measure of how much energy is extracted from a primary nuclear fuel source and is measured as the actual energy released per mass of initial fuel. A Swedish calculated future average burn-up for LWR fuel is in the range 960 to 1080 MWh/kg U (SKB 2010). On discharge from reactor the fuel contains 2 to 6% fission products, depending on the burn-up, and up to 1% of actinides formed by neutron capture and radioactive decay. While each individual fuel bundle or assembly may have a unique irradiation history (in terms of burn-up, power level, and position in reactor) it is not necessary to know the individual characteristics of each bundle/assembly in order to assess its overall long term storage and disposal behavior. For example, for CANDU fuel radionuclide inventories vary very little with power level and can be calculated for a specific burn-up using well developed codes (Tait *et al.* 2000). Based on discharge burn-up distributions, average burn-ups and hence radionuclide inventories, can be calculated and used to determine fuel behavior under storage and disposal conditions.

### CHANGES IN FUEL PROPERTIES DUE TO IN-REACTOR IRRADIATION

UO<sub>2</sub> undergoes a number of microstructural changes due to in-reactor irradiation. Unirradiated fuel possesses a fine-grained, interlocking microstructure with some residual internal sintering porosity from the fabrication process. During in-

reactor irradiation elimination of this porosity, grain growth and the formation of fission gas bubbles trapped at grain boundaries can occur. Depending on linear power rating these bubbles may enlarge and coalesce and eventually lead to the development of gas tunnels along grain boundaries. This evolution in microstructure is illustrated in Figure 11-5.

For LWR (but not CANDU) fuel irradiated at relatively low temperatures (power ratings) the radial variation in grain size and porosity is small, except for a significant increase in porosity around the rim of the fuel pellet where the porosity can be several times higher (to a depth of a few micrometres) than at deeper radial locations. The increased fission rate in this area causes subdivision of the original grains, Figure 11-6, and the increased formation and fission of Pu isotopes increases the burn-up leading to a higher fission product content and alpha activity (Rondinella & Wiss 2010).

The chemical composition and microstructure of nuclear fuel has been studied extensively (Kleykamp 1985, 1988, Kleykamp *et al.* 1985, Hanson 1998). While more than 90% of the fission and activation products and actinides formed remain close to the location of their formation, some redistribution occurs as a consequence of the high operating temperatures. The species formed can be grouped according to their chemical behavior (Johnson *et al.* 1994):

a) Gaseous or somewhat volatile species (He, Kr, Cs, I) migrate within the fuel due to their relatively high diffusion coefficients. A small percentage of these species migrate out of the UO<sub>2</sub> grains into void spaces such as cracks within

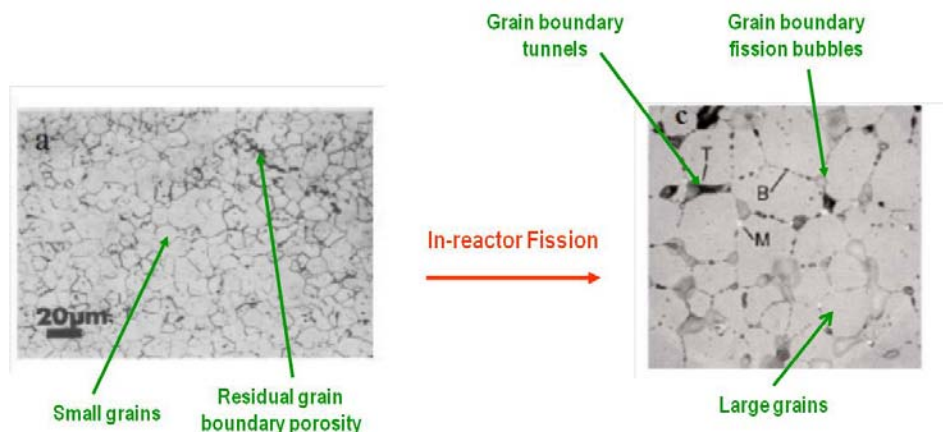


Figure 11-5. Scanning electron micrographs of UO<sub>2</sub> fuel: (a) unirradiated UO<sub>2</sub>; and (b) fuel irradiated at high burn-up (770 MWh/kg U at 52 kW/m). In (a) two key features of the unirradiated fuel are noted. In (b) some of the key features caused by in reactor irradiation are noted.

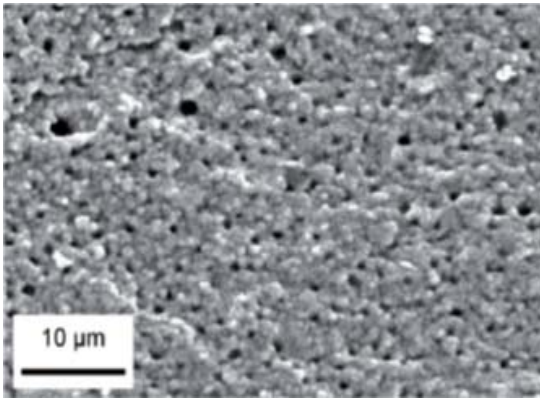


Figure 11-6. Scanning electron micrograph showing the typical structure of the high burn-up rim structure in PWR fuel.

- the fuel and the fuel cladding gap. A somewhat larger percentage segregates to and becomes trapped at grain boundaries within the fuel, while the majority remains trapped as fission gases within the  $\text{UO}_2$  lattice.
- b) Fission products which are non-volatile but unstable as oxides (*e.g.*, Mo, Ru, Pd) can diffuse at high in-reactor temperatures. Small quantities diffuse to grain boundaries to form metallic alloy phases (noble metal ( $\epsilon$ ) particles).
  - c) Fission products which are stable as oxides but incompatible with the  $\text{UO}_2$  matrix (Rb, Cs, Ba, Zn, Nb, Mo, Te, Sr) can separate into secondary precipitates. These phases tend to have the general composition  $\text{ABO}_3$  and to adopt a cubic perovskite-type structure with Ba, Sr and Cs in the A sites and Zn, Mo, U, Pu and rare earths in the B sites (Kleykamp 1985).
  - d) Elements which remain as substitutional ions within the fuel matrix and include actinides (Np, Pu, Am, Cm), the rare earths (La, Ce, Pr, Nd, Pm, Sm, Eu, Gd, Y), and Sr, Zn, Ba, Te and Nb within the limits of their solubility in  $\text{UO}_2$  and to the extent that they have not precipitated in perovskite-type oxides.

Two fission products are worth special mention: Mo, which can be present in both metallic and oxide forms and hence helps to maintain the fuel close to stoichiometry; and Zr, which tends to distribute between perovskite-type phases and the fuel matrix, within which it exerts a major influence on lattice dimensions (Kleykamp 1993). Small inventories of activation products ( $^{14}\text{C}$ ,  $^{59}\text{Ni}$  and  $^{63}\text{Ni}$ ) are also formed in the Zircaloy cladding which experiences an extremely high neutron fluence in the reactor.

Figure 11-7 summarizes this distribution of fission products, activation products and actinides within the spent fuel matrix (Johnson *et al.* 1994).

Based on these studies it is possible to define three categories of radionuclide for which eventual release mechanisms under disposal conditions would be expected to be different (Fig. 11-8):

- (1) The gap inventory, comprising radionuclides released to the fuel cladding gap, which would be expected to be soluble, and released on contact with groundwater.
- (2) The grain boundary inventory, composed of those radionuclides which have segregated to grain boundaries within the fuel. Their release will depend on their chemical nature and the physical and chemical properties of the grain boundaries and could require a protracted period of exposure to groundwater.
- (3) The matrix inventory of radionuclides consisting of species retained within fuel grains and whose release would be controlled by the dissolution properties of the fuel.

Of these categories, (1) and (3) have been extensively studied whereas the determination of grain boundary inventories (2) and properties has

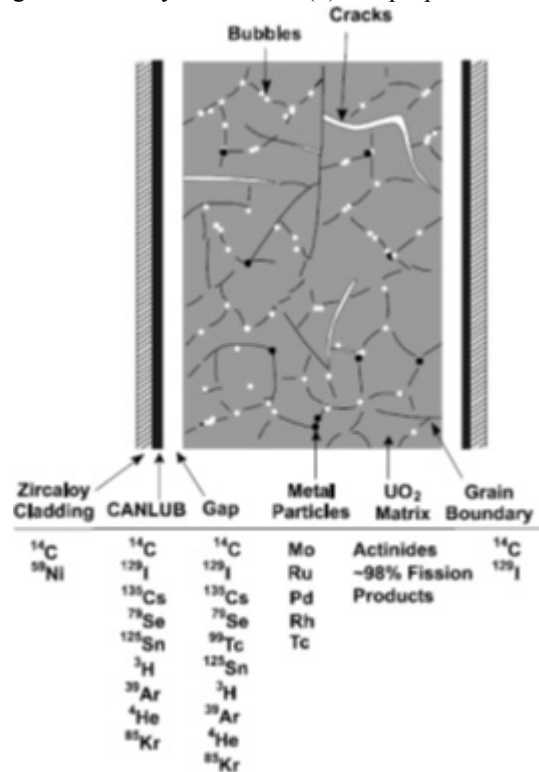


Figure 11-7. Schematic showing the conceptual distribution of fission and activation products within a spent fuel element.

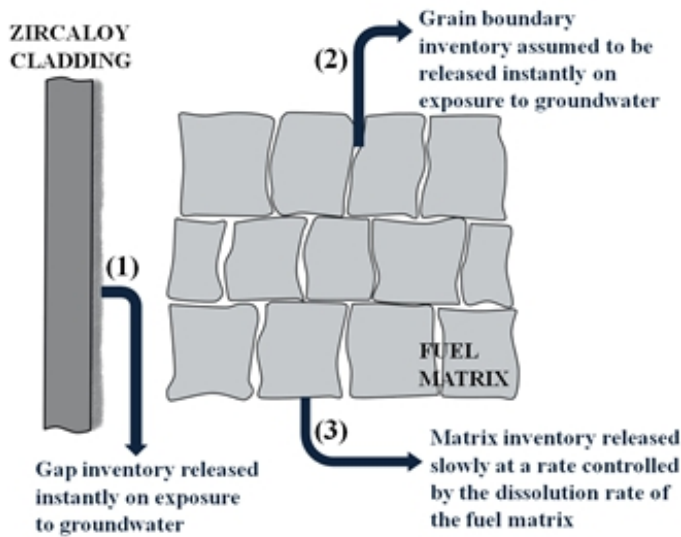


Figure 11-8. Conceptual illustration of the three categories of radionuclide within a spent fuel element.

proven very difficult. As a consequence until demonstrated otherwise, the grain boundary inventory is assumed to be released on contact with groundwater, and only two categories are considered when assessing fuel performance: an instant release fraction (IRF) comprising inventories (1) and (2), and a matrix dissolution fraction (MDF) comprising inventory (3).

On discharge from reactor, the fuel is highly

radioactive, but its activity decreases quickly, Figure 11-9. For CANDU fuel, the overall radioactivity decreases to ~1% of its initial value within a year and to 0.01% after 10 years. During this period the fuel would be stored in water-filled pools at the reactor site (period 1 in Figure 11-9). Beyond this time the fuel could be moved to dry storage (period 2) for presently undefined times up to 100 years or possibly longer. Unless a decision to

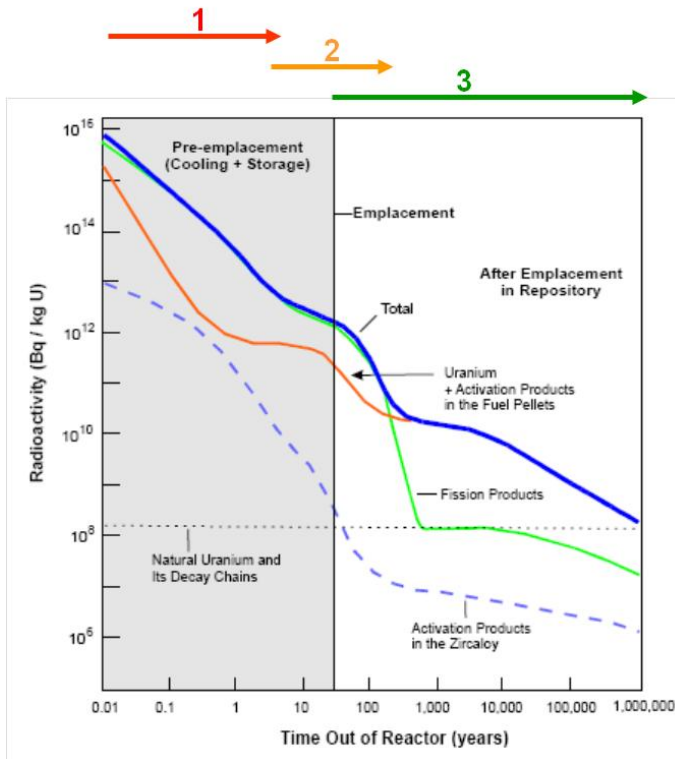


Figure 11-9. Activity associated with CANDU fuel and its variation with time since discharge from reactor: 1, the period when the fuel would be stored in water filled pools at the reactor site; 2, the period when the fuel could be stored dry in a temporary storage facility; 3, the period of interest after permanent disposal in an underground repository.

reprocess the fuel is taken during this period, final disposal in a geologic repository (period 3) would be implemented.

Many of the  $\gamma$ -emitting fission products and the activation products within the cladding would decay rapidly within the first few hundred years (Fig. 11-9). Beyond this period, the decay process would be dominated by the long-lived actinides most of which decay by the emission of alpha particles ( ${}^4\text{He}^{2+}$ ). Beyond  $10^6$  years the radioactivity level approaches that defined by the natural U decay chain ( ${}^{235}\text{U} \rightarrow {}^{207}\text{Pb}$ ; the half-life ( $t_{1/2}$ ) for the first step in this chain is  $7.04 \times 10^8$  years). While the overall decrease in radioactivity is important, of equal importance is the gradual change in radionuclide composition of the fuel since radiotoxicity is related to a specific radionuclide. The importance of any specific radionuclide depends on its inventory in the fuel (g/kg U), its half-life and its radiotoxicity. Figure 11-10 shows the inventories of some key long-lived radionuclides in CANDU fuel. These curves define the repository containment period required for these specific radionuclides. The increase in  ${}^{235}\text{U}$  is due to its formation by the decay of  ${}^{239}\text{Pu}$  ( ${}^{239}\text{Pu} \rightarrow {}^{235}\text{U} + 4\text{He}$ ).

## CHANGES IN FUEL PROPERTIES AFTER DISCHARGE FROM REACTOR

### Radionuclide Diffusion

Since it contains  $\alpha$ -emitters the crystalline structure of  $\text{UO}_2$  could experience  $\alpha$ -recoil damage during storage or after disposal when temperatures would not be high enough to ensure annealing of the damage as would be the case at high in-reactor temperatures. This damage has the potential to increase the rate at which gaseous species diffuse from within the pellet to the fuel-cladding gap, thereby increasing the IRF. For LWR fuel Ferry *et al.* (2005) calculated an upper limit of ~6% for this increase over 10,000 years. The changes are unlikely to be significant for CANDU fuel since the total inventories of mobile elements are much lower.

### Build-up of Helium Pressure

Alpha decay processes within the fuel will produce He gas which, by causing a build-up in pressure, could lead to changes in the microstructure of the fuel. While generally insignificant for CANDU fuel, this is a possibility for LWR fuel especially in the rim region where burn-up will be enhanced. Helium atoms can be trapped in existing fission gas bubbles, form new bubbles, or remain dissolved in the fuel matrix. Using conservative

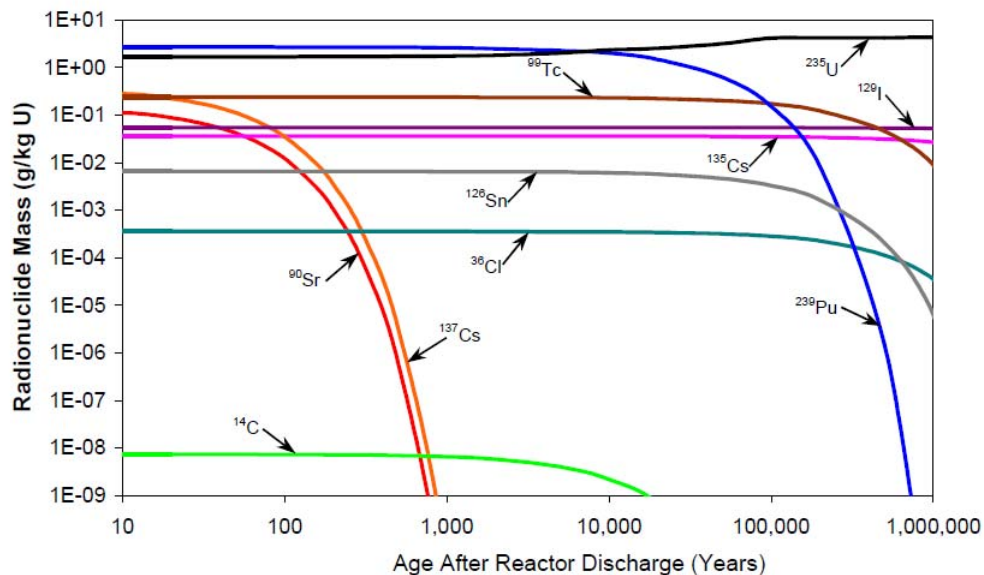


Figure 11-10. Change in inventory of some key long-lived radionuclides over time in spent fuel (220 MWh/kg U).  ${}^{238}\text{U}$  (not shown) is the most abundant radionuclide. The increase in  ${}^{235}\text{U}$  is due to the in-growth from the decay of  ${}^{239}\text{Pu}$ . Most of the radionuclides, including  ${}^{90}\text{Sr}$  and  ${}^{137}\text{Cs}$  and many others that are not shown, decay almost completely within 1,000 years after discharge.

assumptions this build-up has been modeled (Ferry *et al.* 2006, 2010). In spite of these conservatisms, the calculated pressure of He in new or pre-existing bubbles was found to be much lower than the critical values derived from fuel rupture criteria. This makes the rupture of large grains and the propagation of cracks in the rim zone very unlikely within the first  $10^4$  years of disposal.

### FUEL BEHAVIOR UNDER DISPOSAL CONDITIONS

The determination of the behavior of used nuclear fuel under disposal conditions requires the development of a numerical spent fuel (SNF) source term to describe the radionuclide release processes on contact with groundwater after container failure. This source term contains two contributions:

- (1) the instant release fraction (IRF) involving the instantaneous release of the gap and grain boundary inventories;
- (2) the matrix dissolution fraction (MDF) involving the slow release of radionuclides fixed within the fuel matrix.

#### The Instant Release Fraction (IRF)

The determination of the IRF requires knowledge of the radionuclide inventories, the half-lives and decay sequences of the individual radionuclides, and analytical measurements of the gap and grain boundary inventories. The half-lives of most radionuclides are known and tabulated (ICRP 1991) although some important ones (*e.g.*,  $^{79}\text{Se}$  and  $^{126}\text{Sn}$ ) remain uncertain (Chumseng *et al.* 1997, Naas *et al.* 1996). Radionuclide inventories can be determined using well developed codes (*e.g.*, for CANDU fuel (Tait *et al.* 2000), and are

calculated as the best estimate for an average container inventory after a specific decay period since discharge from reactor. This decay period depends on the duration of pool and dry storage (periods 1 and 2 in Figure 11-9) prior to final disposal. The average container inventory is calculated from the distribution of individual fuel bundle or assembly burn-ups for the reactor fuel inventories awaiting disposal.

The gap and grain boundary inventories can be measured by first puncturing the fuel cladding and measuring the fission gas released and then leaching both the clad fuel (to obtain the gap inventory) and the crushed fuel (to obtain the gap + grain boundary inventories). The release fraction of a specific radionuclide expected to be a component of the IRF can then be determined by comparing the amount released to the calculated inventory.

These measurements and calculations have been described in detail (Stroes-Gascoyne *et al.* 1987, 1992a, 1992b, 1994, 1996, Gray *et al.* 1991, Roudil *et al.* 2007, 2009, Johnson & McGinnes 2002, Johnson *et al.* 2005). The release of fission gas is strongly correlated with the linear heat rating. Since at higher burn-ups there is a reduction in fuel thermal conductivity, temperatures are higher leading to an increase in fission gas release at high burn-up (Fig. 11-11). As shown, considerable uncertainty exists in the data at high burn-ups, particularly for MOX fuel. MOX fuel is nuclear fuel containing more than one oxide of fissile material, usually  $\text{PuO}_2$ . The Pu agglomerates in MOX fuel, which have a diameter of  $\geq 10\mu\text{m}$ , experience significantly higher burn-ups than the rest of the fuel and the variability in the quantities of fission gas released and trapped in the porous structure of

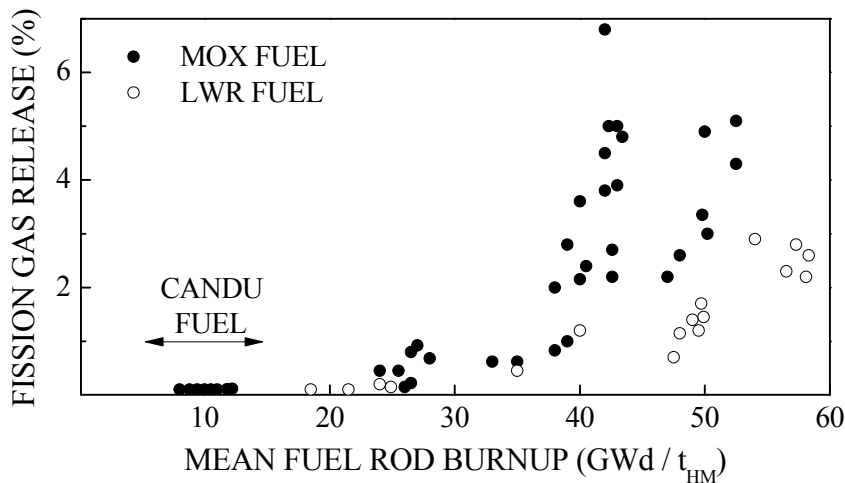


Figure 11-11. Fission gas release from French LWR and MOX fuel as a function of burn-up (taken from Johnson and McGinnes, 2002). The arrow shows the range of burn-ups for CANDU fuel.

the agglomerates leads to these uncertainties (Johnson *et al.* 2005).

For CANDU fuel, which experiences considerably lower burn-ups, the release of the radionuclides  $^{137}\text{Cs}$  and  $^{129}\text{I}$  has been shown to correlate linearly with the fission gas releases, Figure 11-12 (Stroes-Gascoyne *et al.* 1987, Johnson & Shoesmith 1988), indicating equivalent release of these radionuclides. For other radionuclides the IRFs can be obtained from leaching experiments. The IRF values for a number of important radionuclides in CANDU fuel are listed in Table 11-1 (Garisto 2002).

### Matrix Dissolution

The release of the > 90% of radionuclides contained within the solid state matrix of the used fuel will be governed by the corrosion/dissolution of the  $\text{UO}_2$  matrix. The rate of this process will be related to, but not necessarily directly proportional to, the solubility of the U in the groundwater. At repository depths, anticipated groundwater is inevitably oxygen-free and any O introduced during repository construction and operation prior to sealing will be rapidly consumed by mineral and biochemical reactions in the clays in the vicinity of the container (Figures 11-1 and 11-2) and by minor corrosion of the contain material (expected to be Cu or carbon steel (possibly Ti)) depending on the country and geologic formation chosen (King & Shoesmith 2010).

For these neutral anoxic conditions, the theoretical solubility of crystalline  $\text{UO}_2$  calculated

from thermodynamic data is extremely low ( $\sim 10^{-15}$  mol/L) (Neck & Kim 2001). Measurements, however, yield values of the order of  $10^{-9.5}$  for  $\text{pH} > 4$  due to the formation of amorphous  $\text{UO}_2$  during experiments. Above  $\text{pH} = 4$ , the solubility is insensitive to  $\text{pH}$ . Since there is some variation in measured solubilities depending on the crystallinity of the solid, the OECD-NEA recommended value is  $10^{-8.5}$  mol/L (Grenthe *et al.* 1992, Guillaumont *et al.* 2003). If the concentration of dissolved  $\text{U}^{\text{IV}}$  is controlled at the fuel surface by this solubility equilibrium then the fuel dissolution rate will be controlled by diffusive or advective transport of  $\text{U}^{\text{IV}}$  away from the fuel. Early fuel dissolution models focused on such a solubility-limited transport process (*e.g.*, Johnson *et al.* 1994) and the rates of RN release by matrix dissolution were predicted to be very low.

TABLE 11-1. INSTANT RELEASE FRACTIONS (IRF) FOR RADIONUCLIDES IN USED CANDU FUEL

Radionuclide	IRF (% of inventory)
Cs	8
I	8
C	3
Cl	8
Sr	3
Tc	1
Kr	8
Xe	8

Source: Garisto (2002)

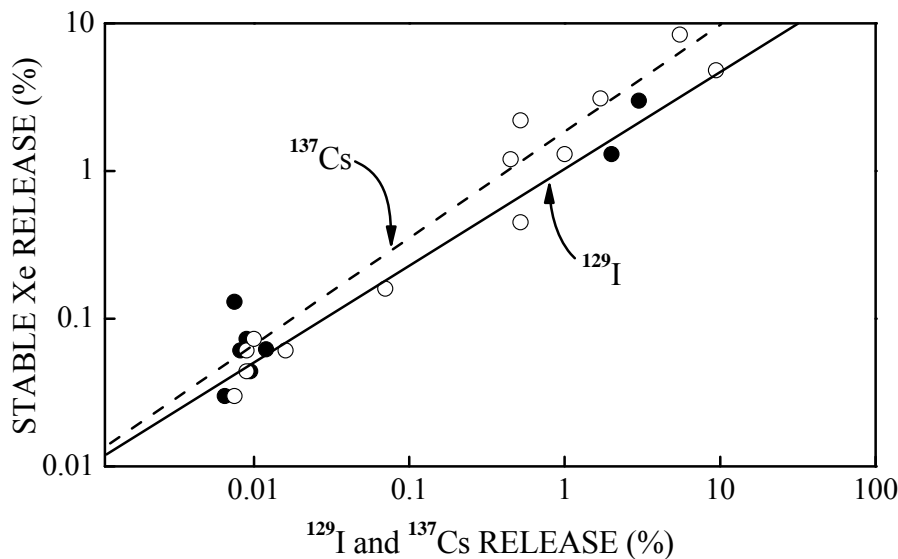


Figure 11-12. Relationship between Xe release during in reactor irradiation and short term leachability of  $^{137}\text{Cs}$  and  $^{129}\text{I}$  (from Johnson & Shoesmith, 1998).

While groundwater entering a failed container may be anoxic, its radiolysis due to radioactive decay processes within the fuel will produce a variety of chemical species including oxidants. These species will be formed directly at, or in the environment immediately adjacent to, the fuel surface once it is wetted with groundwater. This possibility of water radiolysis stimulated a revised approach to fuel corrosion studies and the development of radionuclide release models. Under oxidizing conditions,  $\text{UO}_2$  can be oxidized to the +6 oxidation state (e.g., as  $\text{UO}_2^{2+}$ ) and dissolve since the solubility in the  $\text{U}^{\text{VI}}$  state is many orders of magnitude greater than in the  $\text{U}^{\text{IV}}$  state (Grenthe *et al.* 1992, Fig. 11-13). This constitutes a corrosion reaction in which radiolytic oxidants are cathodically consumed driving the anodic oxidation and dissolution of the fuel as shown schematically in Figure 11-14.

The rate of matrix dissolution will depend on redox conditions (Shoesmith 2000, Carbol *et al.* 2005), and, hence, on the radiation dose rate at the fuel surface (Fig. 11-15). The thermodynamic driving force for fuel corrosion is illustrated in Figure 11-16. The redox potential of the groundwater in the vicinity of the fuel surface (commonly termed,  $E_h$ ) will be established by water radiolysis processes, and the thermodynamic driving force for fuel corrosion will be the difference between  $E_h$  and the equilibrium potential for fuel dissolution ( $(E_e)_{\text{UO}_2/\text{UO}_2^{2+}}$ ). Under these conditions, the fuel will establish a corrosion potential ( $E_{\text{CORR}}$ ) at which the fuel (anodic) dissolution rate, the corrosion rate, will be equal to the rate of oxidant

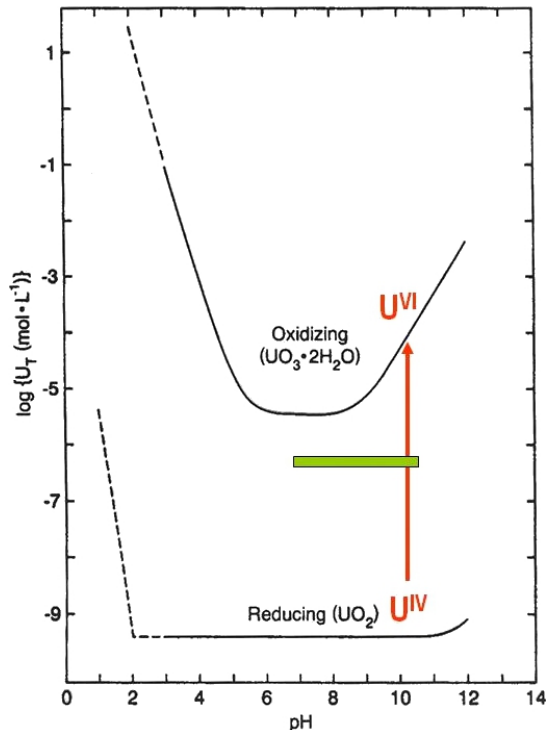


Figure 11-13. Solubilities of  $\text{UO}_2$  and schoepite  $\text{UO}_3 \cdot 2\text{H}_2\text{O}$  as a function of pH at 25°C (plotted from the data in Grenthe *et al.* 1992). The horizontal bar shows the range of pH values expected in spent fuel repositories. The vertical arrow indicates the difference in solubilities between the reduced  $\text{U}^{\text{IV}}$  and oxidized  $\text{U}^{\text{VI}}$  states.

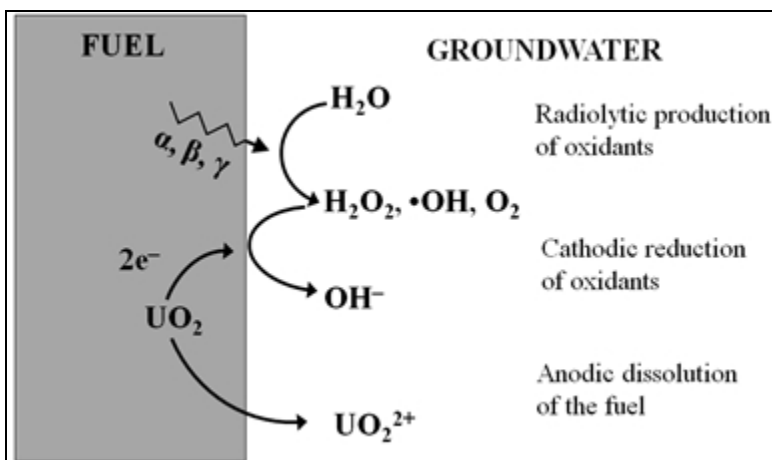


Figure 11-14. Illustration showing the radiolytic production of oxidants by alpha, beta and gamma radiolysis of water, and the coupling of oxidant cathodic processes to anodic fuel dissolution which constitutes the overall fuel corrosion process.

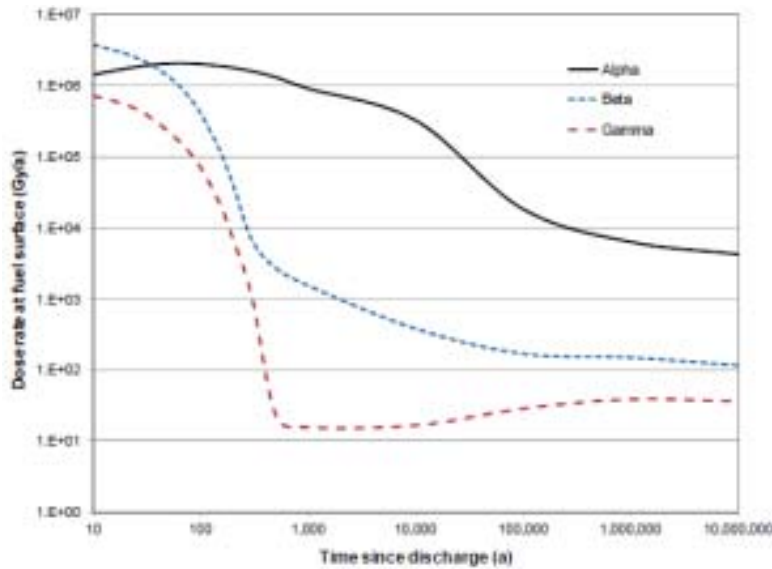


Figure 11-15. Alpha, beta and gamma radiation dose rates as a function of time for a layer of water in contact with a CANDU fuel bundle with a burn-up of 220 MWh/kg U (from He et al.2012).

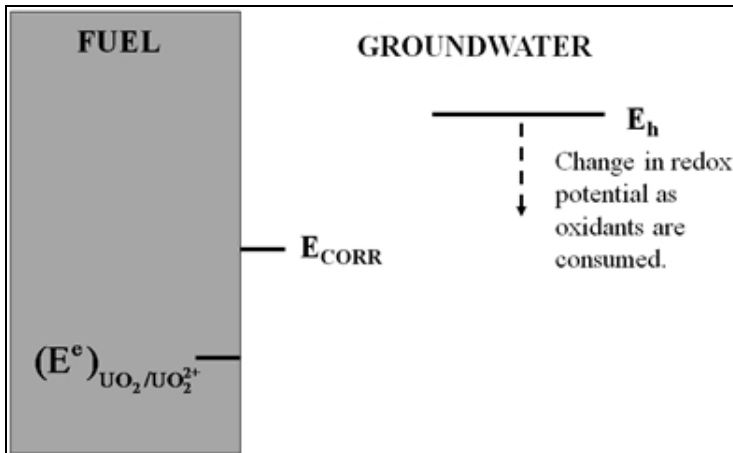


Figure 11-16. Illustration demonstrating the thermodynamic driving force for fuel corrosion in an aqueous solution containing oxidants.  $E_{CORR}$  is the corrosion potential at which the overall corrosion process takes place.

(cathodic) reduction, as illustrated in Figure 11-14.

The radiation fields will decay with time (Figs. 11-9, 11-15) leading to a decrease in radiolytic oxidant concentrations and a decrease in  $E_h$  (Fig. 11-16). This will lead to a decrease in both  $E_{CORR}$  and the fuel corrosion rate until, eventually,  $E_h$  achieves a value  $< (E^e)_{UO_2/UO_2^{2+}}$  when corrosion (as  $U^{VI}$ ) would become thermodynamically impossible and only chemical dissolution (as  $U^{IV}$ ) would be feasible. This evolution makes the corrosion process very dependent on the time to failure of the waste container. Clearly, the longer the period of containment to prevent wetting of the fuel, the lower the rate of production of radiolytic oxidants and, hence, the lower the thermodynamic driving force for fuel corrosion.

### KEY ISSUES INSIDE A FAILED WASTE CONTAINER

The key reactions anticipated within a failed waste container, assumed to be flooded with groundwater, are illustrated in Figure 11-17. The absence of the Zircaloy cladding in this illustration conservatively assumes that the cladding will provide little to no significant protection of the fuel against contact with groundwater and also reasonably assumes it will be inert and chemically uninvolved in the reactions shown.

Two corrosion fronts exist, one on the fuel surface driven by the oxidants produced radiolytically, and a second on the surface of the carbon steel container sustained by the reaction of water to produce  $Fe^{2+}$  and  $H_2$ . In this illustration,  $H_2O_2$  is taken to be the primary radiolytic oxidant

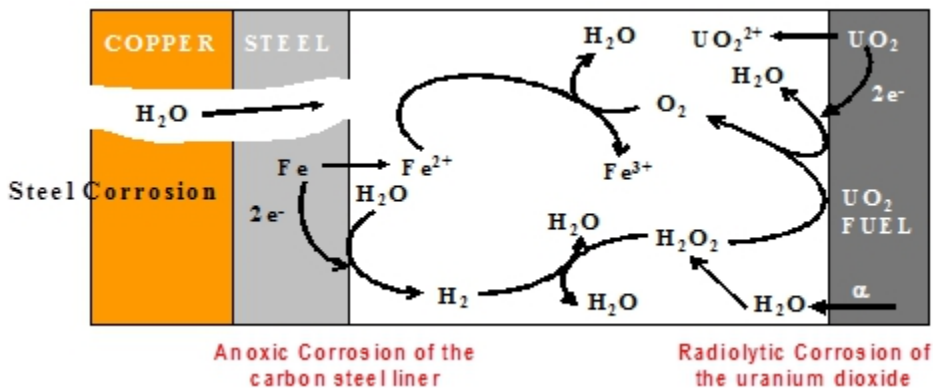


Figure 11-17. Illustration showing the key chemical and electrochemical reactions anticipated inside a failed, groundwater-flooded waste container. A radiolytic corrosion front exists on the fuel surface and an anoxic corrosion front on the surface of the steel vessel.

driving fuel corrosion (Ekeroth *et al.* 2006, Nielsen & Jonsson 2006), although the production of  $O_2$  via  $H_2O_2$  decomposition would introduce a second oxidant. The illustration in Figure 11-18 shows the difference in redox conditions established at these two surfaces, where  $E_h$  is the redox condition which will prevail close to the fuel surface as a consequence of radiolytic  $H_2O_2$  production,  $E^\circ$  are the thermodynamic equilibrium potentials calculated for the reactions indicated, and  $E_{CORR}$  (corrosion potential) values are those measured on  $UO_2$  in  $H_2O_2$  solutions (Shoosmith 2000, Sunder *et al.* 2004) and on the carbon steel/iron under anoxic conditions (Lee *et al.* 2005). The large separation in  $E_{CORR}$  values indicates the likelihood that the products of radiolysis ( $H_2O_2$ ) and steel/iron corrosion ( $Fe^{2+}$ ,  $H_2$ ) will be unstable in each other's presence and on the opposite surfaces to which they are formed.

**SPENT FUEL DISSOLUTION AND RADIONUCLIDE LEACHING**

Many studies of spent fuel dissolution and RN leaching have been performed on different fuel forms with a range of burn-ups under different redox conditions ranging from oxidizing (commonly aerated) to reducing (in the presence of dissolved  $H_2$  or metallic iron/steel which produces  $H_2$  and the additional potential reductant,  $Fe^{2+}$ ) (Jegou *et al.* 2004, 2007, Ekeroth *et al.* 2009, Loida *et al.* 2001, 2009, Glatz *et al.* 2001, Finn *et al.* 1996, Grambow *et al.* 1996, Stroes-Gascoyne *et al.* 1992a, 1992b, Tait *et al.* 1991, Rameback *et al.* 1994, Poinssot *et al.* 2001, Cera *et al.* 2001). These studies have provided the essential database required to define the IRF and to provide information on whether specific radionuclides are released congruently with the dissolving  $UO_2$  fuel matrix. While fuel

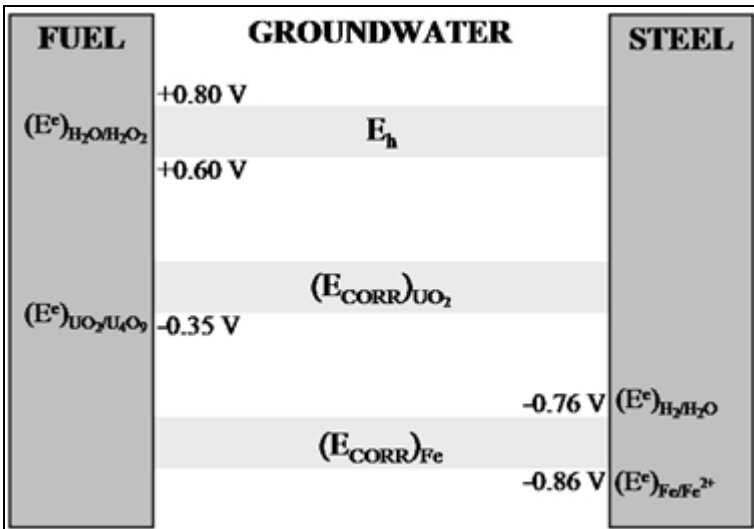


Figure 11-18. Illustration showing the two corrosion conditions existing inside a failed, groundwater-flooded waste container, one on the fuel surface established by reaction with radiolytic oxidants and second one on the steel surface established by reaction with water. The zone marked  $E_h$  indicates the redox condition expected on the fuel surface due to the alpha radiolysis of water. The  $E_{CORR}$  zones indicate the range of values measured on fuel and on steel.

corrosion/dissolution rates are generally quoted as a rate (e.g., in units of  $\text{mg}\cdot\text{d}^{-1}\cdot\text{m}^{-2}$ ), RN release rates are commonly expressed as the fraction of the code-calculated inventory in the aqueous phase (FIAP).

Aside from the need to conduct experiments remotely in a hot cell, there are many complications associated with spent fuel corrosion/dissolution and RN leaching experiments. The physical properties of the fuel are highly variable causing large uncertainties in surface area, an essential parameter to normalize values from different experiments (Iglesias & Quiñones 2008). Additionally, the low solubility of U and many radionuclides makes it easy to exceed solubility limits, a process which buffers solution concentrations by precipitation processes and prevents rate measurements. For this reason, the most reliable rate measurements are achieved using flow-through equipment in which the flow rate of the solution is set sufficiently high to maintain species (particularly U) concentrations below saturation (Rollin *et al.* 2001).

In situations where saturation with U is unavoidable, the release rate of a RN with a high solubility can be used to determine the fuel corrosion/dissolution rate. Generally  $^{90}\text{Sr}$  is used for this purpose since it remains homogeneously distributed within the fuel matrix (Grambow *et al.* 1996) at moderate burn-ups and linear power ratings. At higher burn-ups and linear powers,  $^{90}\text{Sr}$  can be partially segregated to the perovskite phase  $((\text{Ca},\text{Sr},\text{Cs})(\text{U},\text{Pu},\text{Zr},\text{REE})\text{O}_3)$  making it a less reliable dissolution rate monitor.

Figure 11-19 shows an example of fuel corrosion/dissolution rates as a function of pH and redox condition measured using a flow through apparatus (Rollin *et al.* 2001). These experiments were conducted in 10 mM NaCl solution containing

various amounts of HCl and  $\text{NaHCO}_3$  to adjust the pH. In these experiments congruent release was observed for  $^{237}\text{Np}$ ,  $^{90}\text{Sr}$ ,  $^{138}\text{Ba}$ ,  $^{137}\text{Cs}$ ,  $^{99}\text{Tc}$ , and  $^{85}\text{Rb}$  for oxidizing conditions over the whole pH range, although only the fuel corrosion rate calculated from the  $^{137}\text{Cs}$  release are included in the plot. This congruency can be understood by noting that this group of RNs consists of those belonging to the soluble alkali and alkaline earth categories and those which are expected to be redox sensitive producing soluble oxidized species similar to  $\text{UO}_2^{2+}$  ( $\text{NpO}_2^{2+}$ ,  $\text{TcO}_4^-$ ). By contrast, the release of lanthanides (e.g.,  $^{144}\text{Nd}$ ) and trivalent species such as  $^{89}\text{Y}$  and  $^{241}\text{Am}$  were found to depend on pH and carbonate concentration. For the trivalent cations congruent release was observed at pH = 5.7 but insignificant release observed at pH = 6.9. If the solution was Ar-purged the fuel corrosion/dissolution rates decreased by a factor of 5 but RN release continued consistent with the maintenance of oxidizing conditions due to the production of oxidants by water radiolysis.

However, if the solution is purged by  $\text{H}_2$  the dissolution/RN release rates decrease by up to 4 orders of magnitude, Figure 11-19. This influence of  $\text{H}_2$  has been extensively studied on many fuel types including high burn-up PWR and MOX fuel (Carbol *et al.* 2005, 2009a, 2009b, Fors *et al.* 2009, Cui & Spahiu 2011, Cui *et al.* 2008, Grambow *et al.* 1996, Broczkowski *et al.* 2010, Spahiu *et al.* 2002). An influence of  $\text{H}_2$  would also explain the observed suppression of fuel dissolution/RN release rates when steel/iron is allowed to corrode (producing  $\text{H}_2$  and  $\text{Fe}^{2+}$ ) in the same system (Grambow *et al.* 2000). Even millimolar concentrations of dissolved  $\text{H}_2$  lead to almost complete suppression of dissolution/RN release (Carbol *et al.* 2005). Major decreases in release of all RNs are universally

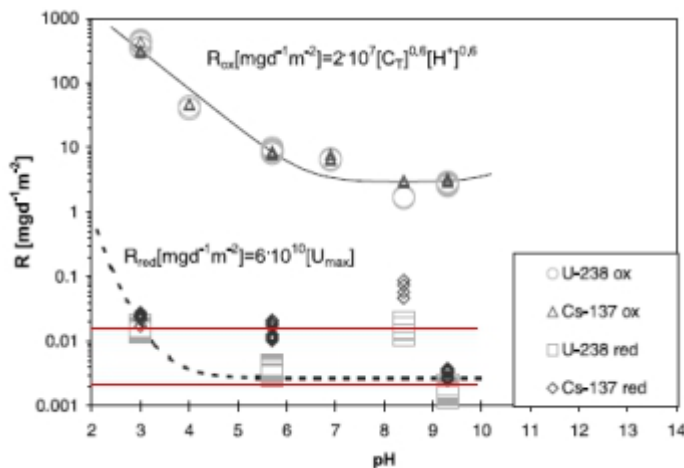
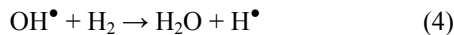


Figure 11-19. Spent fuel dissolution rates as a function of pH for oxidizing and reducing conditions. Oxidizing conditions - solution purged with 20%  $\text{O}_2$  / 0.03%  $\text{CO}_2$  / 80% Ar: $\text{C}_2$  : Reducing conditions - solution bubbled with  $\text{H}_2$  containing 0.03%  $\text{CO}_2$  over a Pt foil (From Rollin *et al.* 2001).

observed and, when analyzed, the concentrations of radiolytic oxidants (specifically  $O_2$ ) in the reaction vessels is well below the detection level ( $\sim 10^{-8}$  mol/L). The measured U concentrations are many orders of magnitude below those calculated for  $U^{VI}$  solids that could reasonably be expected to form in the leaching solutions used (metaschoepite ( $UO_3 \cdot 2H_2O$ ); sodium diuranate ( $Na_2U_2O_7$ )) and at levels which can only be explained by the presence of  $U^{IV}$  solids (Carbol *et al.* 2005).

These results could be explained by the influence of  $H_2$  on the gamma radiolysis of water since even low levels of dissolved  $H_2$  have been shown to suppress the concentrations of molecular radiolytic oxidants to below their detection limit (Pastina *et al.* 1999; Pastina & Laverne 2001). The process involves the scavenging of oxidizing radicals to generate the reducing species  $H^\bullet$ ,



A similar radical scavenging can be invoked for chloride radicals (likely to be an important oxidant in saline repository groundwaters),



This explanation might appear sufficient but experiments performed on unirradiated  $UO_2$  electrodes externally irradiated in a gamma cell in solutions containing  $H_2$  ( $\sim 0.04$  mol/L) show the influence of  $H_2$  is more dramatic than can be explained by just the homogeneous solution scavenging of radiolytic oxidants (King & Shoesmith 2004). In these experiments the corrosion potential ( $E_{CORR}$ ) is suppressed to values well below the thermodynamic threshold for oxidation/corrosion suggesting the  $UO_2$  is rendered immune to corrosion. In addition, when the  $H_2$  is removed  $E_{CORR}$  remains below the threshold suggesting the  $H^\bullet$  radicals produced in reaction (4) have irreversibly reduced the  $UO_2$  surface (King *et al.* 1999).

### Alpha Radiolysis Studies

It seems reasonable to expect that waste containment preventing contact of the fuel with groundwater can be achieved over the time period when gamma( $\gamma$ )/beta( $\beta$ ) radiation fields are significant (Fig. 11-15). This limits the value of corrosion/dissolution rates measured on spent fuels when these radiation fields will be high. Since alpha ( $\alpha$ ) radiation fields persist for considerably longer time periods, the most likely source of oxidants in a failed, groundwater-flooded waste container will be

the products of the  $\alpha$ -radiolysis of water.

With this scenario in mind a considerable effort has been expended on the study of the influence of  $\alpha$ -radiation on  $UO_2$  using predominantly  $\alpha$ -doped  $UO_2$  specimens (usually with either  $^{233}U$  or  $^{238}Pu$ ) (Cobos *et al.* 2002, Rondinella *et al.* 1999, Sattonay *et al.* 2000, Muzeau *et al.* 2009, Stroes-Gascoyne *et al.* 2002, Odegaard-Jensen & Oversby 2008) but also external  $\alpha$ -sources (Sunder *et al.* 1997, Shoesmith *et al.* 2000, Sunder *et al.* 1990, Wren *et al.* 2005). The  $\alpha$ -activity of spent fuel is very dependent on fuel type and burn-up as illustrated in Figure 11-20 for PWR and MOX fuel. A comparison of fuel corrosion/dissolution rates from a wide range of studies involving spent fuel and  $\alpha$ -doped unirradiated  $UO_2$  shows a clear trend of increasing corrosion rate with increasing  $\alpha$ -activity (Fig. 11-21). The sources of the data in this figure are given in Carbol *et al.* (2005) and the data for the  $10^{-2}$  MBq/g( $UO_2$ ) are for unirradiated  $UO_2$  containing no added  $\alpha$ -emitters. The lines drawn in this figure are to emphasize the rate dependence. The two sets of data lying outside this region are for electrochemically determined values recorded on highly resistive  $UO_2$  pellets (high values) and for rates measured in clay environments known to contain reducing species (low values).

As indicated by the lines in this figure there appears to be a specific activity threshold below which no significant influence of  $\alpha$ -radiolysis can be detected. This concept is illustrated schematically in Figure 11-22. Above the threshold fuel corrosion would be radiolytically controlled at a rate determined by the  $\alpha$ -activity, while below the

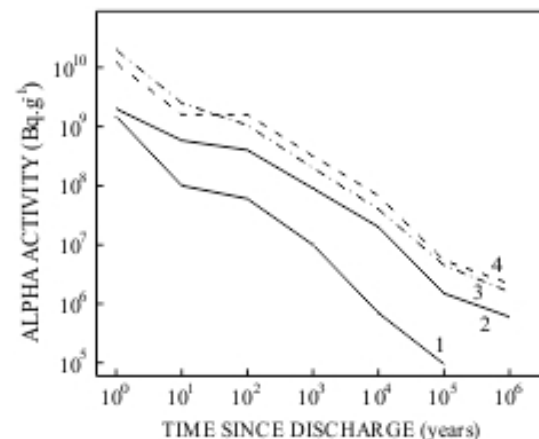


Figure 11-20. Alpha activity of different spent fuels as a function of time since discharge from reactor: 1,  $UO_2$  (36 GWd/tM); 2,  $UO_2$  (60 GWd/tM); 3, MOX (25 GWd/tM); 4, MOX (45 GWd/tM).

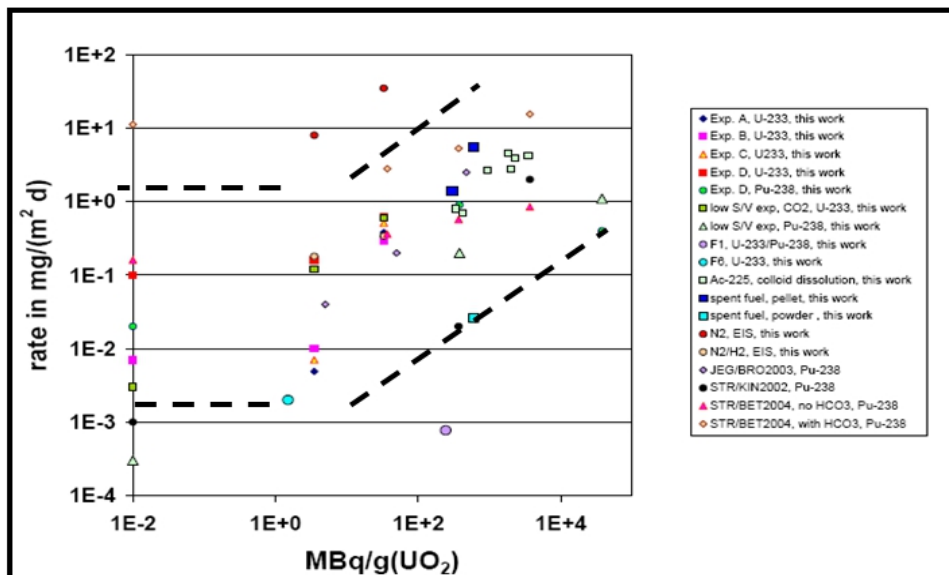


Figure 11-21. Corrosion rates measured for alpha-doped  $UO_2$ , non-doped  $UO_2$  (0.01 MBq/g and spent fuel specimens as a function of alpha activity (Poinssot *et al.* 2005). The sources of the individual data points are given in the reference. The dashed lines are drawn to emphasize the approximate alpha-strength below which no influence of alpha radiation is detectable.

threshold dissolution would be a chemical process proceeding under solubility control. Solubility control was assumed to be established when dissolved U concentrations were  $< 10^{-9}$  mol/L (comparable to the OECD–NEA recommended value of  $10^{-8.5}$  mol/L for the solubility of  $UO_2$ ),  $E_h$  values  $< -0.01V$  (vs SHE) and the observation in long term experiments that the U concentration did not increase with time.

As in the case of spent fuel, the presence of  $H_2$  suppressed the radiolytic corrosion of  $\alpha$ -doped  $UO_2$ ,

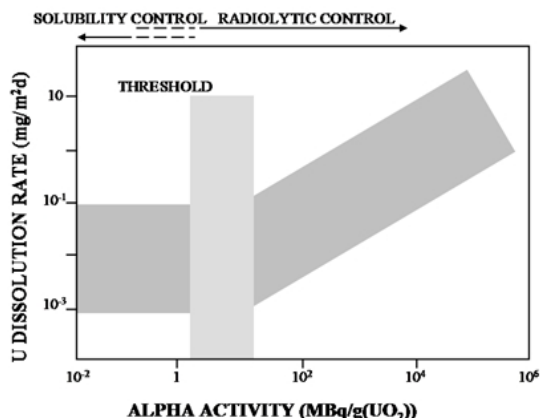


Figure 11-22. Illustration showing the concept of an alpha activity threshold for the onset of radiolytically controlled fuel corrosion. The darker shaded area shows the spread in measured rates from Figure 11-21.

the concentration of dissolved  $H_2$  required depending on the  $\alpha$ -activity in the fuel. An example of such an experiment is shown in Figure 11-23 which shows the influence of changing the dissolved  $H_2$  concentration on the corrosion rate of 10%  $^{233}U$ -doped  $UO_2$  (Carbol *et al.* 2005). All the indicators that corrosion was completely suppressed are present:

- (a) The U concentration is extremely low ( $\leq 10^{-10}$  mol/L) indicating solubility control over the full  $> 2$  year duration of the experiment. In fact, since no change in U concentration occurred over the duration of the experiment, no rate could be calculated.
- (b) Measured  $O_2$  concentrations were in the region of  $10^{-8}$  mol/L which is many orders of magnitude below the amount radiolytically produced.
- (c) The absence of any oxidation of the  $UO_2$  surface was confirmed by X-ray photoelectron spectroscopy (XPS), which is consistent with previous XPS analyses on  $UO_2$  surfaces exposed to external  $\alpha$ -radiation sources in the presence of  $H_2$  (Sunder *et al.*, 1990).

In the absence of  $\gamma$ -radiation, this influence of  $H_2$  cannot be totally attributed to homogeneous solution-scavenging of oxidizing radical species. Considerable discussion on how  $\alpha$ -radiation activates dissolved  $H_2$  to enforce reducing conditions has been published (Carbol *et al.* 2005; Broczkowski *et al.* 2010) but no firm conclusion

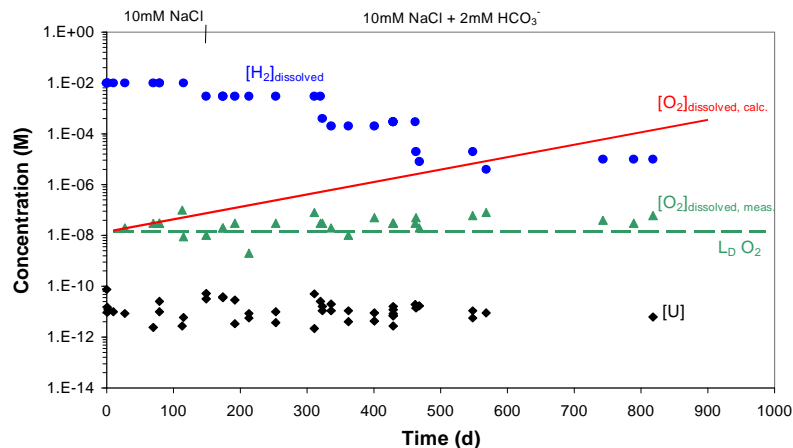


Figure 11-23. Measured  $\text{H}_2$ ,  $\text{O}_2$  and total U concentrations, as a function of time, in a pressure vessel leaching experiment of a 10%  $^{233}\text{U}$ -doped  $\text{UO}_2$  in  $10^{-2}$  mol/L NaCl (0 to 114 days) and  $10^{-2}$  mol/L NaCl +  $2 \times 10^{-2}$  mol/L  $\text{HCO}_3^-$  (114 days onwards) as the  $\text{H}_2$  overpressure was periodically changed. The red line is illustrative only to indicate that the radiolytic  $\text{O}_2$  concentration should increase with time (Carbol *et al.* 2005).

reached. A speculative possibility is that alpha emission produces surface defects by the preferential ejection of the lighter O atom leading to reduced  $\text{U}^{\text{III}}$  states in the fuel surface. Subsequent oxidation of the surface by  $\text{H}_2\text{O}$ , leading to the reincorporation of  $\text{O}^{\text{II}}$  would yield a proton and leave an available  $\text{H}^\bullet$  available to scavenge radiolytic oxidants.

#### CHEMISTRY/ELECTROCHEMISTRY INSIDE A FAILED CONTAINER

Figure 11-17 very briefly outlined the chemistry anticipated within a failed container. A more complete description of the possible reactions has been given elsewhere (Shoesmith *et al.* 2003). Based on this scheme, and calculations and sensitivity analyses performed using a model developed to describe it (Shoesmith 2007, and references therein), the following key issues were identified:

- (i) the composition and chemical/electrochemical reactivity of the fuel surface as a function of redox conditions;
- (ii) the influence of groundwater species and corrosion product deposits on the fuel surface in accelerating or retarding corrosion;
- (iii) the kinetics of  $\text{H}_2\text{O}_2/\text{O}_2$  reduction in support of fuel corrosion;
- (iv) the scavenging of radiolytic oxidants and/or the inhibition of their reaction with the fuel surface by the products of steel/iron corrosion.

These issues have been investigated extensively and reviewed elsewhere (Shoesmith *et al.* 2004, Shoesmith 2007, He *et al.* 2012).

#### Fuel Corrosion Threshold

The dependence of fuel corrosion rate on redox conditions is now well established based on the spent fuel and  $\alpha$ -doped  $\text{UO}_2$  studies described above as well as on unirradiated  $\text{UO}_2$  and simulated spent fuels (Shoesmith 2000, Shoesmith & Sunder 1991; Shoesmith *et al.* 1998, Ekeroth & Jonsson (2003), Hossain *et al.* 2006, Gimenez *et al.* 1996, de Pablo *et al.* 1996, 2001, 2004) and measurements in the presence of radiation fields (Sunder *et al.* 1992, Christensen *et al.* 1994, Shoesmith & Sunder 1992, Jegou *et al.* 2005, Ekeroth *et al.* 2006, Roth & Jonsson 2009, Nilsson & Jonsson 2011, Eriksen *et al.* 2012). Thermodynamically, it is straightforward to define the fuel surface redox conditions when  $\text{UO}_2$  should be immune to corrosion and susceptible only to chemical dissolution. Based on available data (Grenthe *et al.* 1992, Paquette & Lemire 1991),  $E_h$  (and hence  $E_{\text{CORR}}$ ) (Fig. 11-16) would have to be  $< -0.35\text{V}$  (*vs* SCE) at a groundwater pH of 9.5 (and would decrease by 60 mV for each unit increase in pH).

To establish an experimental basis for the interpretation of the influence of various redox reagents, the composition of the fuel surface has been mapped (using XPS) as a function of applied electrochemical potential (Fig. 11-24; Santos *et al.* 2004). The increasing degree of oxidation of the surface above the thermodynamic threshold is clear. All three oxidation states of U are detected and their relative proportions vary with applied potential (Santos *et al.* 2004, Broczkowski *et al.* 2007a, 2007b).

Based on this, and additional electrochemical

evidence, the evolution of fuel surface composition can be specified as a function of potential (Fig. 11-25). In this plot the potential axis is labeled  $E_{\text{CORR}}$  and represents the response of the fuel surface to the redox condition ( $E_h$ ) in the environment. The vertical dashed line is conservatively drawn at  $-0.4\text{V}$  to represent the threshold for the onset of fuel corrosion. Above this potential fuel corrosion will proceed at a rate controlled by the concentration of radiolytic oxidants (specifically  $\text{H}_2\text{O}_2$ ); below this threshold, fuel dissolution and hence the mobilization of RN, can only occur by chemical dissolution,



A parallel can be drawn between this electrochemically established threshold and that demonstrated for  $\alpha$ -activity (Fig. 11-20). Also indicated in Figure 11-25 is the influence of  $\text{H}_2$  on  $E_{\text{CORR}}$  measured in experiments involving  $\gamma$ -radiation (King & Shoesmith 2004), confirming the ability of  $\text{H}_2$  to render the fuel immune to corrosion, at least when  $\gamma$ -radiation is present.

Further inspection of Figures 11-24 and 11-25 shows that, over the potential range from the corrosion threshold to  $\sim 0$  mV (the actual value depends somewhat on temperature) the  $\text{U}^{\text{V}}$  content of the  $\text{U}^{\text{IV}}_{1-2x}\text{U}^{\text{V}}_{2x}\text{O}_{2+x}$  layer increases. As indicated by the arrow marked A in Figure 11-25, this is the potential range expected within a failed container (neglecting any effect of  $\text{H}_2$ ). Since the conductivity of  $\text{UO}_{2+x}$  increases with  $x$  (Hyland and Ralph 1983, Winter 1989) and a surface comprising mixed  $\text{U}^{\text{IV}}/\text{U}^{\text{V}}$  states has been shown to be catalytic for  $\text{O}_2$  reduction (Hocking *et al.* 1994) and involved in  $\text{H}_2\text{O}_2$  reduction (Goldik *et al.* 2005), this change in composition has the potential to influence the corrosion kinetics of the fuel. Attempts to define how the catalytic properties of the  $\text{UO}_{2+x}$  surface change within this potential range have only been partially successful (He *et al.* 2009).

### Reactivity of the Fuel Surface

Measurements of  $\text{UO}_2$  corrosion/dissolution rates (Shoesmith 2000, Oversby 1999) show wide variations in fuel reactivity. In many cases it is unclear whether these differences are attributable to real variations in  $\text{UO}_2$  reactivity or to differences in surface area, experimental conditions and specimen treatment. However, early reports of differences of a factor of  $10^3$  in measured dissolution currents (in electrochemical experiments) for single crystals and sintered discs (Nicol & Needes 1973) and between

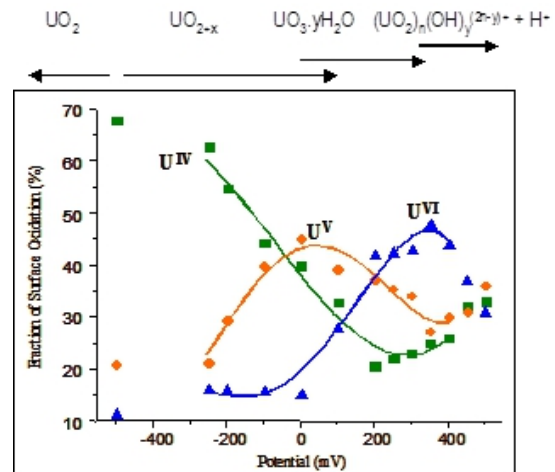


Figure 11-24. The fractions of various oxidation states of U in a 1.5 at.% SIMFUEL electrode surface as a function of applied electrochemical potential. The electrode was anodically oxidized at each potential for 1 hour in 0.1 mol/L NaCl (pH = 9.5) and then analyzed by XPS (Santos *et al.* 2004).

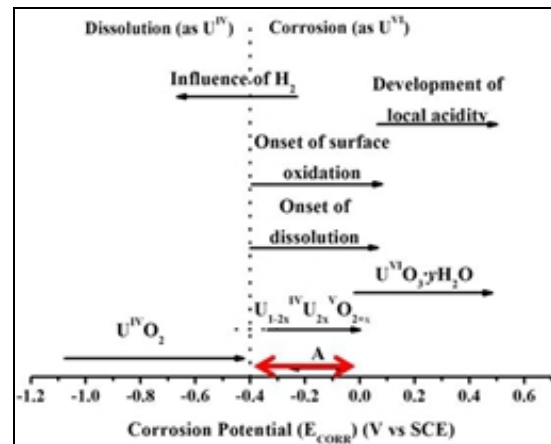


Figure 11-25. The composition of a  $\text{UO}_2$  surface as a function of corrosion potential (from Figure 11-24). The vertical dashed line indicates the potential threshold above which  $\text{UO}_2$  would be expected to be subject to corrosion, and below which only chemical dissolution can occur. The arrow A indicates the corrosion potential range anticipated inside a failed waste container.

$\text{UO}_2$  and natural uraninite samples containing ill-defined impurities (Grandstaff 1976) suggested that the presence of defects and impurities introduced during in-reactor fission exert significant effects on corrosion rates.

While it is impossible to simulate in unirradiated  $\text{UO}_2$  all the features which could influence the corrosion rate, the key ones can be reproduced in custom made SIMFUELS ( $\text{UO}_2$  doped

with specific stable elements to simulate the chemical effects of in-reactor burn-up (Lucuta *et al.* 1991) or otherwise-doped  $\text{UO}_2$  specimens. Figure 11-26 illustrates the key changes induced by in-reactor irradiation which would be expected to change the reactivity of the fuel under disposal conditions and which can be simulated in unirradiated  $\text{UO}_2$  fuel analogs: (i) rare earth doping of the  $\text{UO}_2$  matrix; (ii) the presence of noble metal ( $\epsilon$ ) particles; and (iii) residual non-stoichiometry (though not necessarily in grain boundaries).

Considerable evidence exists to show that the fission products and actinide–lanthanide doping of the fuel associated with burn-up stabilizes the fuel against air oxidation (Thomas *et al.* 1993, Choi *et al.* 1996, Cobos *et al.* 1998, McEachern & Taylor 1998) and preliminary electrochemical and chemical studies on SIMFUELS and rare earth-doped  $\text{UO}_2$  suggest a similar influence in aqueous environments (He *et al.* 2007, Pehrman *et al.* 2012).

Hyperstoichiometry exerts a major influence on the electronic conductivity of  $\text{UO}_2$ . In the stoichiometric form,  $\text{UO}_2$  is a Mott-Hubbard insulator with a filled narrow 5f band, containing two electrons per U atom, located in the  $\sim 5$  eV gap between the filled valence band and the empty conduction band (Shoesmith *et al.* 1994). The introduction of non-stoichiometry, in the form of incorporated additional  $\text{O}^{\text{II}}$  ions, accompanied by the creation of  $\text{U}^{\text{V}}$  atoms to maintain charge balance creates holes in the 5f level making the electrical conductivity of  $\text{UO}_{2+x}$  very sensitive to the degree of non-stoichiometry. In addition, non-stoichiometric locations have been shown to provide donor-acceptor  $\text{U}^{\text{IV}}/\text{U}^{\text{V}}$  sites which catalyze the cathodic

reduction of radiolytic oxidants (Hocking *et al.* 1994, Goldik *et al.* 2005) and hence could accelerate fuel dissolution, as illustrated schematically in Figure 11-27.

Non-stoichiometry has also been shown to exert a major influence on  $\text{UO}_2$  reactivity (He *et al.* 2012) and references thesis). Micro Raman spectroscopy showed very distinct changes in fuel structure occur as  $x$  (in  $\text{UO}_{2+x}$ ) increases (He & Shoesmith 2010 and references therein). At low degrees of non-stoichiometry there is an increase in the number of randomly distributed O interstitial defects. As the degree of non-stoichiometry increases these defects associate into clusters, and for a sufficiently high degree of non-stoichiometry cuboctahedral clusters are formed (He & Shoesmith 2010, Desgranges *et al.* 2012, and references therein).

Studies using atomic force microscopy (AFM), current sensing-AFM and scanning electrochemical microscopy (He *et al.* 2012 (and references therein)) clearly demonstrated that the fuel reactivity increased substantially with highly non-stoichiometric clusters being  $\geq 10^3$  more reactive than close-to-stoichiometric  $\text{UO}_2$ . While the exact mechanistic details of the anodic oxidation mechanism remain unresolved, the extent of oxidation on a surface close to stoichiometry appears to be limited by the low O interstitial mobility within the matrix. At higher degrees of non-stoichiometry the formation of defect clusters enhances O interstitial mobility in the matrix but may limit the overall degree of surface oxidation, Figure 11-28.

While this increase in reactivity was correlated with the locations of corrosion damage, an exact

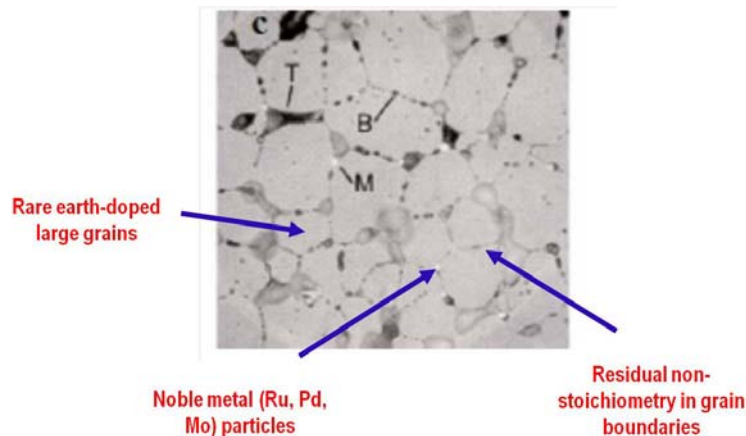


Figure 11-26. Scanning electron micrograph of irradiated fuel (burn-up 770 MWh/kgU at 52 kW/m). The features noted are those changes due to in-reactor irradiation which are expected to have the most significant influences on fuel corrosion and can be simulated in unirradiated  $\text{UO}_2$  specimens.

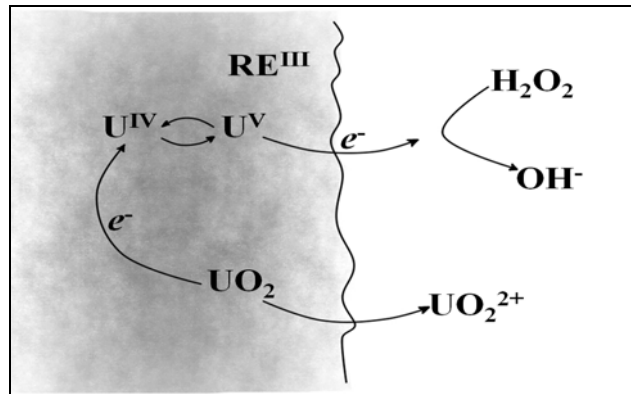


Figure 11-27. Illustration showing  $\text{H}_2\text{O}_2$  reduction is catalyzed by donor-acceptor ( $\text{U}^{\text{IV}}/\text{U}^{\text{V}}$ ) sites on the surface of rare earth (RE)-doped  $\text{UO}_2$ .

measure of the influence of non-stoichiometry on corrosion kinetics has not been obtained. Since the degree of non-stoichiometry is unlikely to increase in-reactor to beyond  $\text{UO}_{2.007}$ , these studies suggest the potential influence on spent fuel corrosion rate should be less than a factor of 5, and is likely to be considerably lower than this. However, since non-stoichiometry may occur predominantly in grain boundaries, it is judicious to retain the presently adopted assumption (in waste disposal performance assessment calculations) that RNs residing in grain boundaries will be part of the IRF.

#### Influence of Corrosion Product Deposits

Since fuel corrosion is likely to persist for long periods of time (unless inhibited by  $\text{H}_2$ ) the accumulation of corrosion product deposits is a possibility. Any such accumulation could have a number of effects:

- (i) It could suppress corrosion by blocking the fuel surface to an extent determined by the porosity of the deposit, as shown schematically in Figure 11-29.
- (ii) It could restrict the diffusive mass transport of species to and from the reacting surface (Fig. 11-29). Since the primary oxidant driving fuel corrosion,  $\text{H}_2\text{O}_2$ , is produced by radiolysis at the fuel surface, a sufficiently thick, low porosity deposit could prevent diffusive loss of  $\text{H}_2\text{O}_2$  from surface sites. Such a deposit would also hinder the access of the redox scavengers  $\text{Fe}^{2+}$  and  $\text{H}_2$  to the corroding surface, thereby reducing the efficiency of scavenging. A model which attempts to incorporate this scenario (Shoesmith *et al.* 2003) predicts that, in the absence of scavenging by  $\text{H}_2$ , effectively 100% of the radiolytic  $\text{H}_2\text{O}_2$  would be consumed by fuel corrosion. This model should be considered conservative.

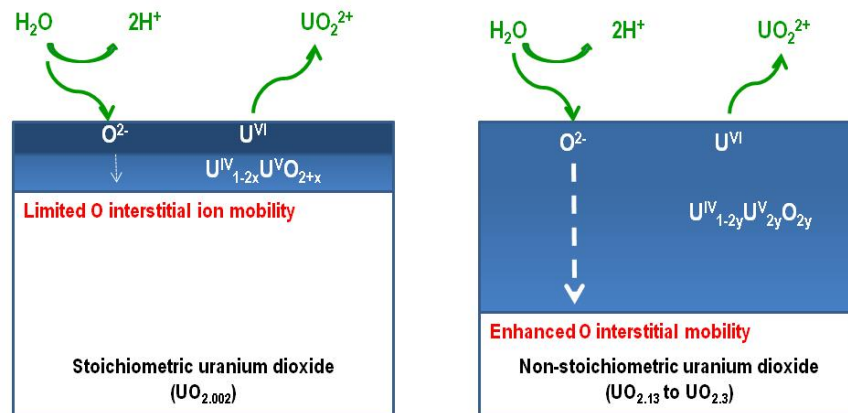


Figure 11-28. Illustrations showing the influence of non-stoichiometry on the electrochemical oxidation kinetics of  $\text{U}^{\text{IV}}_{1-2x}\text{U}^{\text{V}}_{2x}\text{O}_{2+x}$ . The increase in O interstitial ion mobility with increasing  $x$  leads to deeper oxidation but a lesser degree of oxidation at the oxide/solution interface.

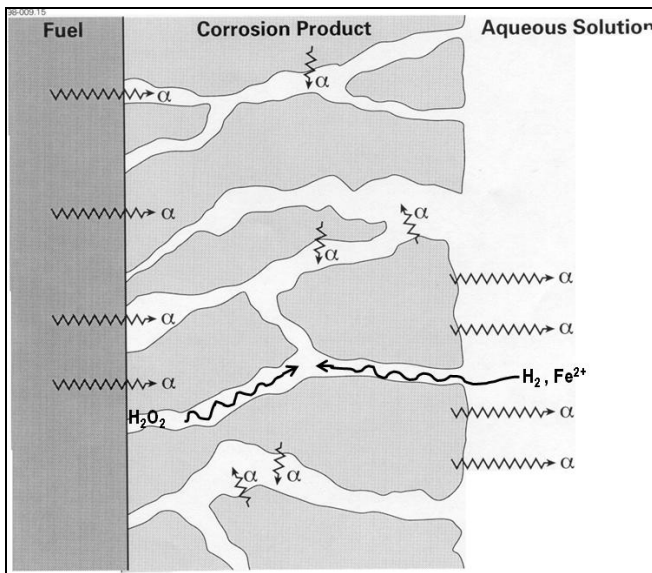


Figure 11-29. Illustration of a corrosion product layer on a corroding  $\text{UO}_2$  surface illustrating the continuous network of connected pores, the transport of radiolytically-produced  $\text{H}_2\text{O}_2$  and  $\text{H}_2$  and  $\text{Fe}^{2+}$  produced by corrosion of the steel/iron container, and the redistribution of  $\alpha$ -emitting radionuclides from the fuel to the corrosion product as corrosion proceeds.

(iii) Deposits could incorporate radionuclides (Fig. 11-29) especially actinides such as Np (Burns *et al.* 1997a, Buck *et al.* 1998, Finch *et al.* 2002, Burns *et al.* 2004). While this would prevent, or at least delay, their release to groundwater it would modify the yield and distribution of  $\alpha$ -radiolysis products (Fig. 11-29).

The influence of deposits is difficult to study on a laboratory time frame since their rate of accumulation under corrosion/dissolution conditions is very slow, especially when redox conditions are only slightly oxidizing. Similarities in the alteration phases (redeposited dissolved U solids) observed in laboratory experiments and in the geological alteration of natural uraninite deposits (Buck *et al.* 1997, Wronkiewicz *et al.* 1996, Finch *et al.* 1999) provides evidence that the overall alteration processes observed in the laboratory under oxidizing conditions are similar to those likely to control alteration under oxidizing repository conditions.

The studies show that the groundwater species  $\text{Ca}^{2+}$  and silicates are readily incorporated into  $\text{U}^{\text{VI}}$  alteration phases such as becquerelite ( $\text{Ca}(\text{UO}_2)_6\text{O}_4(\text{OH})_6 \cdot 8\text{H}_2\text{O}$ ), soddyite ( $(\text{UO}_2)_2\text{SiO}_4 \cdot 2\text{H}_2\text{O}$ ), weeksite ( $(\text{K}_2(\text{UO}_2)_2\text{Si}_6\text{O}_{15} \cdot 4\text{H}_2\text{O})$ ), boltwoodite ( $(\text{Na,K})(\text{UO}_2)(\text{SiO}_3\text{OH}) \cdot \text{H}_2\text{O}$ ), and  $\beta$ -uranophane ( $\text{Ca}(\text{UO}_2)_2(\text{SiO}_3\text{OH})_2 \cdot 5\text{H}_2\text{O}$ ). In addition, dissolution experiments using flow-through apparatus to avoid precipitation processes show that these two species interfere directly with the corrosion process, the rate being decreased by a factor of up to 200 with the larger influence being exerted by the silicate (Shoesmith 2000). A special feature of

corrosion in the presence of the water radiolysis product  $\text{H}_2\text{O}_2$  is the possibility of forming studtite ( $\text{UO}_4 \cdot 4\text{H}_2\text{O}$ ) or metastudtite ( $\text{UO}_4 \cdot 2\text{H}_2\text{O}$ ). These phases have been found in nature (Kubatko *et al.* 2003), and observed in spent fuel leaching (Hanson *et al.* 2005) and  $\text{UO}_2$  dissolution (Clarens *et al.* 2004) experiments. It has also been shown (Forbes *et al.* 2011) that the conversion of phases such as schoepite and soddyite to studtite is kinetically facile. Whether or not studtite/metastudtite will be significant alteration phases at the low  $\text{H}_2\text{O}_2$  concentrations due to  $\alpha$ -radiolysis remains to be demonstrated. Since these phases are unstable in the absence of  $\text{H}_2\text{O}_2$  they would only be expected if containers failed while  $\alpha$ -radiation fields were significant.

For the initially slightly oxidizing to long-term anoxic conditions anticipated in deep geologic repositories, the investigation of the influence of corrosion product films is considerably more difficult. Attempts to analyze alteration products on the surface of fuel specimens exposed to solutions containing  $\text{Ca}^{2+}$  and silicate were unsuccessful although the formation of coffinite ( $\text{USiO}_4 \cdot n\text{H}_2\text{O}$ ) was suspected and minor amounts of ekanite ( $(\text{U,Ca})_2\text{Si}_8\text{O}_{20}$ ) may have formed (Amme *et al.* 2005). While by themselves inconclusive, these observations are consistent with analyses from the Cigar Lake deposit (Saskatchewan, Canada) where reducing conditions were maintained (Cramer & Smellie 1994). The mixed  $\text{U}^{\text{IV}}\text{U}^{\text{VI}}$  solid ianthinite ( $\text{U}^{\text{IV}}(\text{U}^{\text{VI}}\text{O}_2)_5(\text{OH})_{14} \cdot 3\text{H}_2\text{O}$ ) has been observed under oxidizing conditions (Burns *et al.* 1997b), but appeared to form as a consequence of the local

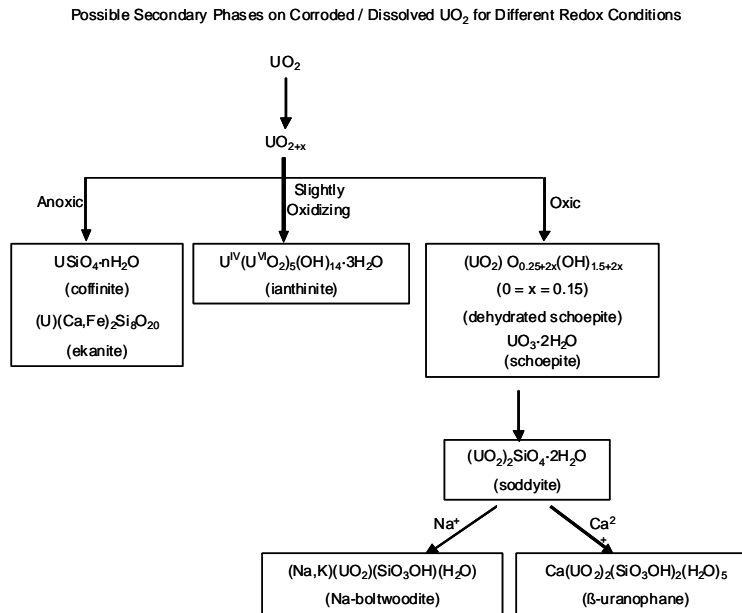


Figure 11-30. Possible secondary phases that could form on a corroding fuel surface under oxidizing conditions and on a chemically dissolving surface under anoxic conditions.

depletion of oxidants at the sites at which it was observed. Figure 11-30 summarizes the possible evolution of alteration phases under different redox conditions based on these studies (Santos *et al.* 2006). Since the mineralogy of U is extremely complex especially under oxidizing conditions (Wronkiewicz 1999), these sequences are only representative illustrations and not an exhaustive list of possibilities.

While  $\text{Ca}^{2+}$  and silicate are the species most likely to promote the formation of deposits the groundwater species most likely to prevent it are  $\text{HCO}_3^-/\text{CO}_3^{2-}$  by complexation of the  $\text{UO}_2^{2+}$  dissolution product (Grenthe *et al.* 1992), which leads to an increase in  $\text{U}^{\text{VI}}$  solubility and the acceleration of the dissolution kinetics. Both electrochemical (Shoesmith 2007, Keech *et al.* 2011) and chemical studies (de Pablo *et al.* 1996, Hossain *et al.* 2006, de Pablo *et al.* 1999, Ilin *et al.* 2001, Cobos *et al.* 2003) yield consistent results. When the total of  $\text{HCO}_3^-/\text{CO}_3^{2-}$  concentration is  $\geq 10^{-3}$  mol/L which is possible under anticipated groundwater conditions, formation of  $\text{U}^{\text{VI}}$  deposits is prevented and corrosion proceeds uninhibited at a rate considerably greater than in the presence of carbonate. As the carbonate concentration is increased,  $\text{HCO}_3^-/\text{CO}_3^{2-}$  not only prevents deposition, but inhibits formation of the underlying  $\text{U}^{\text{IV}}_{1-2x}\text{U}^{\text{V}}_{2x}\text{O}_{2+x}$  layer, Figure 11-24 (de Pablo *et al.* 1996, Hossain *et al.* 2006) and catalyzes fuel

dissolution via a surface complexation process (Keech *et al.* 2011).

The influence of  $\text{HCO}_3^-/\text{CO}_3^{2-}$  on the kinetics of fuel dissolution decreases with decreasing applied potential indicating that any kinetic influence of these anions on fuel corrosion will become insignificant as anoxic conditions are approached. Additionally, as their concentration decreases below  $10^{-4}$  mol/L their ability to prevent corrosion product deposition decreases (Hossain *et al.* 2006).

### Kinetics of $\text{H}_2\text{O}_2$ Reduction

The kinetics of  $\text{H}_2\text{O}_2$  reduction have been investigated in detail using electrochemical (Shoesmith 2007 and references therein) and chemical techniques (Gimenez *et al.* 1996, de Pablo *et al.* 2001, Hossain *et al.* 2006, Shoesmith 2000, Nilsson & Jonsson 2011, Hossain & Jonsson 2008), and shown to occur considerably faster than the reduction of  $\text{O}_2$ . This higher rate can be attributed to the ability of  $\text{H}_2\text{O}_2$  to rapidly create its own  $\text{U}^{\text{IV}}/\text{U}^{\text{V}}$  donor-acceptor sites rather than rely on the number of such sites pre-existing in the fuel surface, as is the case of  $\text{O}_2$  reduction, Figure 11-31. The creation of such sites would also be expected to catalyze  $\text{H}_2\text{O}_2$  decomposition, as illustrated in Figure 11-31, and claims that decomposition occurs have been advanced (Diaz-Arocas *et al.* 1995, Amme 2002, Amme *et al.* 2002, Lousada *et al.* 2012).

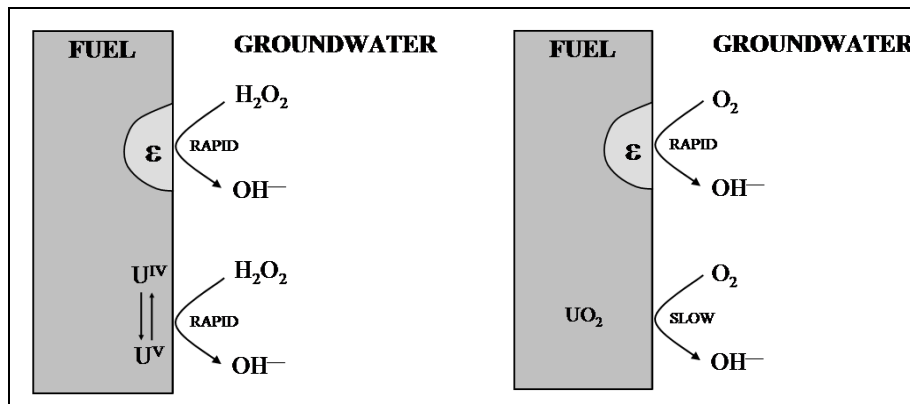
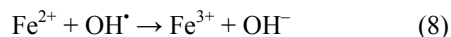
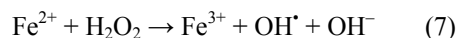


Figure 11-31. Illustrations showing that H<sub>2</sub>O<sub>2</sub> reduction is rapid on both the UO<sub>2</sub> surface and on noble metal (ε) particles, while the reduction of O<sub>2</sub> is rapid only on the particles. The ability of H<sub>2</sub>O<sub>2</sub> to oxidize the fuel surface and create U<sup>IV</sup>/U<sup>V</sup> donor-acceptor sites makes its reduction rapid on both the fuel and the particle, making the kinetics difficult to separate experimentally. By contrast, the inability of O<sub>2</sub> to similarly create donor-acceptor sites means the kinetics of its reduction on particles is much faster than on the fuel surface, making the two reactions easily separable.

As was previously observed for O<sub>2</sub> reduction (Hocking *et al.* 1994, Shoesmith 2000, 2007), H<sub>2</sub>O<sub>2</sub> reduction can also be catalyzed on the noble metal (ε) particles present in SIMFUEL and spent fuel as illustrated in Figure 11-31. This could lead to an increase in corrosion rate, but this could be partly counterbalanced by the ability of these particles to catalyze H<sub>2</sub>O<sub>2</sub> decomposition to the much slower reacting oxidant, O<sub>2</sub> (Nilsson & Jonsson 2011).

### The Influence of Redox Scavengers

As illustrated in Figure 11-17, fuel corrosion/radionuclide release will occur inside a container also undergoing corrosion, to produce the potential redox scavengers, Fe<sup>2+</sup> and H<sub>2</sub>. Ferrous ion is a well-known regulator of redox conditions in natural waters and its reaction with oxidants, in particular dissolved O<sub>2</sub>, has been extensively studied (Stumm 1990). Hydrogen peroxide will be consumed by the Fenton reaction (Jonsson *et al.* 2006, Sutton *et al.* 1989),



Studies on the influence of Fe and Fe corrosion products on fuel corrosion have been published (Shoesmith *et al.* 2003, Loida *et al.* 1996, Grambow *et al.* 1996, El Aamrani *et al.* 1998, Loida *et al.* 2006, Albinsson *et al.* 2003, Cui *et al.* 2003, Quiñones *et al.* 2001, Ollila *et al.* 2003, Stroes-Gascoyne *et al.* 2002a, 2002b) and inevitably show that the presence of Fe suppresses corrosion and RN release. Measurements over a period of 4.5 years demonstrated a reduction in <sup>90</sup>Sr release rate by a

factor of 460. In experiments with <sup>233</sup>U-doped UO<sub>2</sub>, U concentrations were lower than the solubility limit when Fe was present (Ollila *et al.* 2003).

It is not possible to separate the scavenging effects of Fe<sup>2+</sup> and H<sub>2</sub> in experiments with Fe/steel since both are produced its corrosion. More direct attempts have been made to determine the influence of Fe<sup>2+</sup> on fuel corrosion both experimentally (Quiñones *et al.* 2001, Ollila *et al.* 2003) and via model calculations (Jonsson *et al.* 2006, King *et al.* 2002). Addition of Fe<sup>2+</sup> to experiments with Pu-doped electrodes (Stroes-Gascoyne *et al.* 2002a, 2002b) showed that while an [Fe<sup>2+</sup>] of 10<sup>-5</sup> mol/L did not influence E<sub>CORR</sub> a concentration of 10<sup>-4</sup> mol/L suppressed it by 0.14V suggesting a direct influence on the concentration of radiolytically produced oxidants. Calculations based on experimentally determined rate constants (Jonsson *et al.* 2006) indicate that the consumption of H<sub>2</sub>O<sub>2</sub> via the Fenton reaction ([Fe<sup>2+</sup>] = 1 μmol/L) leads to a substantial suppression of UO<sub>2</sub> dissolution (> a factor of 40). By contrast, calculations using an electrochemical model (King *et al.* 2002) indicate only a minor effect. The difference between these two calculations is the presence of a corrosion product deposit in the latter, but not the former, calculation. This deposit acts as a diffusion barrier limiting access of dissolved Fe<sup>2+</sup> to the fuel surface where the H<sub>2</sub>O<sub>2</sub> is radiolytically produced, as illustrated in Figure 11-29.

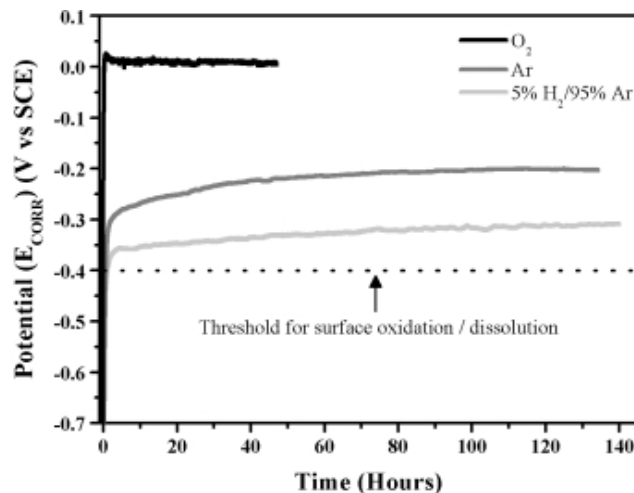
As described above the suppression of fuel corrosion and RN release in the presence of H<sub>2</sub> is very large and has been recently reviewed (Carbol *et al.* 2005, Broczkowski *et al.* 2010). The expected

steel corrosion rates of 0.05 to 0.1  $\mu\text{m}/\text{year}$  (Smart *et al.* 2002a, b) would lead to the establishment of  $\text{H}_2$  pressures  $> 5 \text{ MPa}$  in a sealed repository (Carbol *et al.* 2005) and dissolved groundwater concentrations in the 10 to 100 mmol/L range.

While the mechanism by which  $\text{H}_2$  is activated by  $\gamma$ - and  $\alpha$ -radiation may be uncertain, there is no doubt about this mechanism on noble metal ( $\epsilon$ ) particles. This process has been electrochemically (Broczkowski *et al.* 2005, 2006, 2007a, 2007b) and chemically (Nilsson & Jonsson 2007) characterized using SIMFUEL specimens with different levels of simulated burn-up (*i.e.*, different number densities of particles) or added Pd particles. The  $E_{\text{CORR}}$  on SIMFUELS is very responsive to redox conditions, and even small amounts of dissolved  $\text{H}_2$  suppress the value to well below those measured under purely anoxic conditions, Figure 11-32. The value is also very dependent on the number density of  $\epsilon$ -particles, a SIMFUEL simulating 6 at.% burn-up (equivalent to a high burn-up PWR fuel) suppressing  $E_{\text{CORR}}$  to the potential threshold for corrosion, Figure 11-33. XPS analyses confirmed that the extent of surface oxidation varied with  $E_{\text{CORR}}$  and that the  $\text{UO}_2$  surface was unoxidized at the potential threshold value. Even a moderate increase in  $\text{H}_2$  pressure (*i.e.*, dissolved  $[\text{H}_2]$ ) suppressed  $E_{\text{CORR}}$  to values below the threshold rendering the  $\text{UO}_2$  immune to corrosion.

This effect can be attributed to the reversible dissociation of  $\text{H}_2$  to  $\text{H}^\cdot$  radicals on the noble metal particles which protect the galvanically coupled  $\text{UO}_2$  matrix from corrosion, as illustrated schematically in Figure 11-34.

This galvanic coupling is aided by the increased conductivity of the  $\text{UO}_2$  matrix due to rare-earth doping. Since noble metals are catalytic for both the



reduction of fuel oxidants, *e.g.*,  $\text{H}_2\text{O}_2$  as well as the reductant  $\text{H}_2$  as illustrated in Figure 11-35, it is not surprising that it can be shown that  $\epsilon$ -particles will

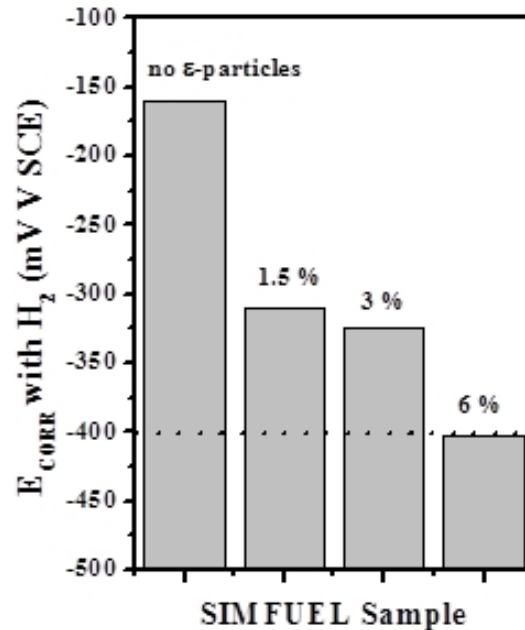


Figure 11-33. The influence of the increasing number and size of noble metal ( $\epsilon$ ) particles in SIMFUELS with different degrees of simulated burn-up (expressed as at.%) on the corrosion potential ( $E_{\text{CORR}}$ ) measured in  $\text{H}_2/\text{Ar}$  purged 0.1 mol/L (pH = 9.5) at 60°C. The horizontal line shows the threshold for corrosion (from Figure 11-25) (Shoesmith 2007).

Figure 11-32. Corrosion potential measurements on a 1.5 at.% SIMFUEL surface in 0.1 mol/L KCl (pH = 9.5) solution purged with various gases at 60°C. The electrode was electrochemically-cleaned prior to the start of each experiment. The dashed line shows the potential threshold for corrosion (from Figure 25) (Broczkowski *et al.* 2005).

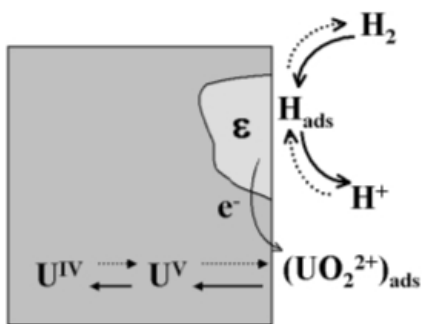


Figure 11-34. Illustration showing the galvanic coupling of  $\epsilon$ -particles to the fuel matrix allowing  $\text{H}_2$  oxidation on the particle to suppress fuel oxidation.

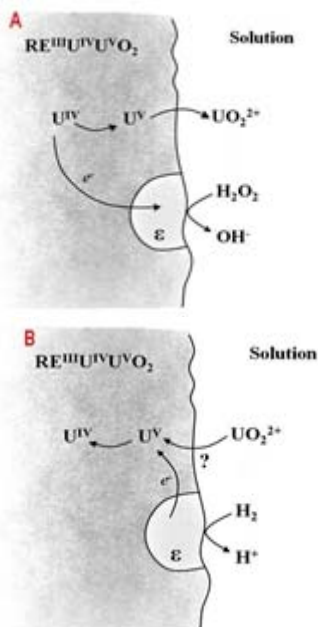


Figure 11-35. Illustrations showing how noble metal ( $\epsilon$ ) particles dispersed throughout a conducting, rare-earth-doped  $\text{UO}_2$  matrix could catalyze (A) oxidant reduction reactions leading to the acceleration of corrosion, and (B) reductant oxidation reactions leading to the suppression of corrosion. The question mark in (B) indicates that there is no substantial evidence that  $\text{H}_2$  oxidation can reverse the corrosion reaction by driving the redeposition of dissolved  $\text{UO}_2^{2+}$ .

also catalyze the reaction between  $\text{H}_2\text{O}_2$ , and  $\text{H}_2$  to produce  $\text{H}_2\text{O}$  (Nilsson & Jonsson 2007, Broczkowski *et al.* 2010). This was demonstrated in  $\text{H}_2/\text{Ar}$  purged solutions to which  $\text{H}_2\text{O}_2$ , was added and shown to be consumed without causing corrosion. That surface oxidation could be avoided (or reversed) when the SIMFUEL contained  $\epsilon$ -particles, but not when they were absent, was confirmed by XPS and cathodic stripping voltammetry (Broczkowski *et al.* 2010).

These experiments clearly demonstrate that the presence of small amounts of dissolved  $\text{H}_2$  can both suppress  $\text{UO}_2$  oxidation and catalyze  $\text{H}_2\text{O}_2$  scavenging even on simulated fuel containing low densities of  $\epsilon$ -particles (*i.e.*, with the simulated burn-up expected for low burn-up CANDU fuel). Since the radiolytic concentrations of  $\text{H}_2\text{O}_2$  produced by  $\alpha$ -radiolysis are expected to be many orders of magnitude ( $10^6$  to  $\geq 10^8$ ) less than the concentrations of  $\text{H}_2$  trapped in a sealed repository, it is possible that the fuel corrosion/RN release process could be completely suppressed by  $\text{H}_2$  oxidation on noble metal particles. Preliminary model calculations suggest  $[\text{H}_2]$  concentrations of  $\leq 10^{-4}$  mol/L would be sufficient (Wu *et al.* 2012).

### CHEMICAL DISSOLUTION RATES

Based on the above studies there is a strong probability that the corrosion of spent fuel can be avoided either by long term containment in a sealed container or by the reducing influence of  $\text{H}_2$  in a failed container. Under the latter condition chemical dissolution will be the only mechanism for matrix dissolution leading to the release of the great majority of the radionuclides retained within the spent fuel matrix. Figure 11-36 shows a series of estimates of the chemical dissolution rates taken from a number of sources. In this figure, the solid horizontal line is the selected best estimate ( $2.4 \times 10^6$  mol/m<sup>2</sup>.a). The dashed lines suggest upper and lower bounds.

The compiled data are from the following sources:

- (1) The corrosion rates compiled by Poinssot *et al.* (2005) for  $\text{UO}_2$  specimens with low specific activity (*i.e.*,  $<0.01$  MBq  $\text{UO}_2$  in Figure 11-21). At this activity level it is claimed that dissolution is chemical not radiolytic.
- (2) The corrosion rates predicted by extrapolation of a simple electrochemical model to the corrosion threshold defined in Figure 11-25. Below this threshold dissolution should be chemical not electrochemical.
- (3) Grambow & Giffaut (2006) claimed that the dissolution rate of spent fuel under reducing conditions is  $<0.01$  mg  $\text{UO}_2/\text{m}^2\text{d}$ .
- (4) The data taken from Ollila (2007).
- (5) Values given by Salah *et al.* (2006) measured in Belgium Boom clay. These values were recorded on  $\alpha$ -doped specimens but no influence of  $\alpha$ -activity was observed. This is thought to be due to the reducing conditions imposed by organic reductants in the clay. If this is the case, then

chemical dissolution would be expected to prevail.

- (6) The value recommended by Grambow *et al.* (2010) in the final report of the ECC Mikado project.
- (7) The used fuel dissolution rates measured by Rollin *et al.* (2001) in the presence of H<sub>2</sub> gas (Figure 11-19). Commonly no rate can be measured when H<sub>2</sub> is present. Since rates could be measured it is assumed that there was just enough H<sub>2</sub> to suppress corrosion and that the dissolution observed was approaching the maximum chemical dissolution rate.

The selected best estimate is based on the assumption that some of the data (particularly 1 and 7) are overestimates, and takes into account that 6 is the most carefully considered and selected value.

### SUMMARY

Based on extensive studies a detailed understanding of fuel dissolution processes is now available. This is especially true for the oxidizing (corrosive) conditions produced by the radiolysis of water. However, an understanding of the chemical dissolution process expected once radiation fields have decayed is not yet well characterized. This is not surprising since this process is expected to be very slow, uranium in the +4 oxidation state being very insoluble. Other possible alteration processes, which could apply under non-oxidizing conditions, such as the alteration of the fuel to coffinite

(USiO<sub>4</sub>,H<sub>2</sub>O), are not well understood, even the thermodynamics being in doubt.

A considerable effort has been expended in defining the release rates of different categories of radionuclide. A reasonable semi-quantitative description of what is termed the instant release fraction (IRF) is now available. These estimates are, however, very conservative for some radionuclides since they include an ill-defined contribution from radionuclides presumed to reside at grain boundaries. Presently, there is little to no information available on the behavior of these locations in the fuel.

More basic laboratory studies have developed a comprehensive understanding of the chemistry/electrochemistry likely to occur inside a failed container. The presence of two conflicting corrosion fronts, radiolytic corrosion of the fuel and anoxic corrosion of the carbon steel container, is now well established, and a considerable amount of evidence exists that the interference of these two processes could lead to a very significant suppression of fuel corrosion and radionuclide release. However, at present no convincing measure of how effective this process will be is available. Any such evaluation would necessarily have to include the influence of fuel cladding in allowing these two corrosion fronts to interact. Presently, the influence of the cladding is generally ignored since it is not expected to influence the chemistry inside the container. This may not be quite the conservative assumption it is taken to be.

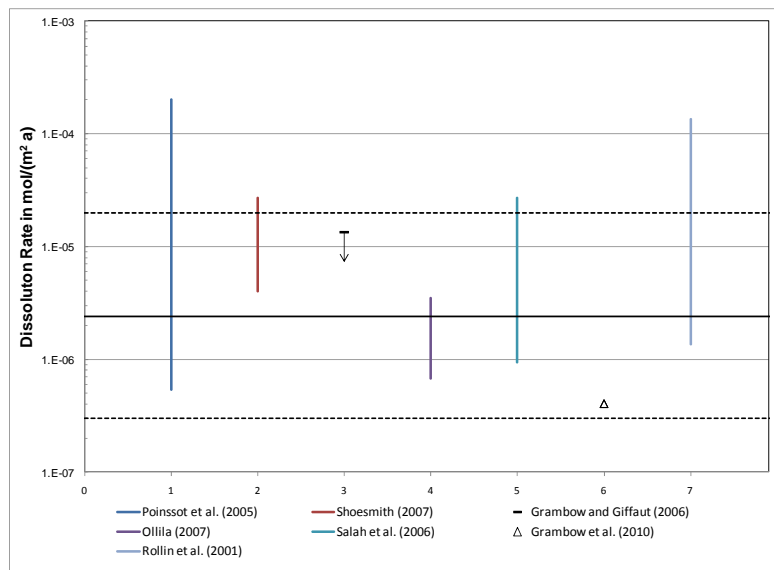


Figure 11-36. UO<sub>2</sub> corrosion rates from various literature sources. The solid line is the best estimate chemical dissolution rate and the dashed lines are the selected upper and lower bounds.

**ACKNOWLEDGEMENT**

This review was written under the Industrial Research Chair agreement between the Canadian Natural Sciences and Engineering Research Council (NSERC), the Nuclear Waste Management Organization (NWMO) and Western University.

**REFERENCES**

- ALBINSSON, Y., ODEGAARD-JENSEN, A., OVERSBY, V.M. & WERME, L.O. (2003): Leaching of spent fuel under anaerobic and reducing conditions. *Mat. Res. Soc. Symp. Proc.* 757, 407-413.
- AMME, M. (2002): Contrary effects of the water radiolysis product H<sub>2</sub>O<sub>2</sub> upon the dissolution of nuclear fuel in natural groundwater and deionized water. *Radiochim. Acta* 90, 399-406
- AMME, M., RENKER, B., SCHMID, B., FETH, M.P., BERTAGNOLLI, H. & DOBELIN, W. (2002): Raman microspectrometric identification of corrosion products found on UO<sub>2</sub> nuclear fuel during leaching experiments. *J. Nucl. Mater.* 306, 202-212.
- AMME, M., WISS, T., THIELE, T., BOULET, P. & LANG, H. (2005): Uranium secondary phase formation during anoxic hydrothermal leaching processes of UO<sub>2</sub> nuclear fuel. *J. Nucl. Mater.* 341, 209-223.
- BENNETT, D.G. & GENS, R. (2008): Overview of European concepts for high-level waste and spent fuel disposal with special reference to waste container corrosion. *J. Nucl. Mater.* 379, 1-8.
- BROCZKOWSKI, M., NOEL, J.J. & SHOESMITH, D.W. (2005): The inhibiting effects of hydrogen on the corrosion of uranium dioxide under nuclear waste disposal conditions. *Nucl. Mater.* 346, 16-23
- BROCZKOWSKI, M., NOEL, J.J. & SHOESMITH, D.W. (2006): The influence of temperature on the anodic oxidation/dissolution of uranium dioxide. *Electrochim. Acta* 52, 7386-7395.
- BROCZKOWSKI, M.E., NOËL, J.J. & SHOESMITH, D.W. (2007a): Corrosion of uranium dioxide containing simulated fission products in dilute hydrogen peroxide and dissolved hydrogen. *J. Electrochem. Soc.* 157, C275-281.
- BROCZKOWSKI, M.E., NOEL, J.J. & SHOESMITH, D.W. (2007b): The influence of temperature on the anodic oxidation/dissolution of uranium dioxide. *Electrochim. Acta* 52, 7386-7395.
- BROCZKOWSKI, M., ZAGIDULIN, D. & SHOESMITH, D.W. (2010): The role of dissolved hydrogen on the corrosion/dissolution of spent nuclear fuel. *In: Nuclear Energy and the Environment*, Chien M. Wai and Bruce J. Mincher (Eds). *American Chemical Society Symp. Proc.* 1046, Chapter 26, 349-380.
- BUCK, E.C., WRONKIEWICZ, D.J., FINN, P.A. & BATES, J.K. (1997) A new uranyl oxide hydrate phase derived from spent fuel oxidation. *J. Nucl. Mater.* 249, 70-76.
- BUCK, E.C., FINCH, R.J., FINN, P.A. & BATES, J.K. (1998): Retention of neptunium alteration phases during spent fuel corrosion. *Mat. Res. Soc. Symp. Proc.* 506, 83-89.
- BURNS, P.C., EWING, R.C. & MILLER, M.L. (1997a): Incorporation mechanisms of actinide elements into the structure of U<sup>VI</sup> phases formed during the oxidation of spent nuclear fuel. *J. Nucl. Mater.* 245, 1-9.
- BURNS, P.C., FINCH, R.J., HAWTHORNE, F.C., MILLER, M.L. & EWING, R.C. (1997b): The crystal structure of Ianthinite, [U<sub>2</sub><sup>4+</sup>(UO<sub>2</sub>)<sub>4</sub>O<sub>6</sub>(OH)<sub>4</sub>(H<sub>2</sub>O)<sub>4</sub>](H<sub>2</sub>O)<sub>5</sub>: a possible phase for Pu<sup>4+</sup> incorporation during the oxidation of spent nuclear fuel. *J. Nucl. Mater.* 249, 199-206.
- BURNS, P.C., DEELY, K.M. & SKANTHAKUMAR, S. (2004): Neptunium incorporation into uranyl compounds that formed as alteration products of spent nuclear fuel. Implications for geologic repository performance. *Radiochim. Acta.* 93, 151-160.
- CARBOL, P., COBOS-SABATE, J., GLATZ, J.-P., RONCHI, C., RONDINELLA, V., WEGEN, D.H., WISS, T., LOIDA, A., METZ, V., KIENZLER, B., SPAHIU, K., GRAMBOW, B., QUIÑONES, J. & MARTINEZ ESPARZA VALIENTE, A. (2005): The effect of dissolved hydrogen on the dissolution of <sup>233</sup>U-doped UO<sub>2</sub>(s), high burn-up spent fuel and MOX fuel, Swedish Nuclear Fuel and Waste Management Company, Technical Report TR-05-09.
- CARBOL, P., FORS, P., GOUDER, T. & SPAHIU, K. (2009a): Hydrogen suppresses UO<sub>2</sub> corrosion. *Geochim. Cosmochim. Acta* 73, 4306-4375.
- CARBOL, P., FORS, P., VAN WINCKEL, S. & SPAHIU, K. (2009b): Corrosion of irradiated MOX fuel in presence of dissolved H<sub>2</sub>. *J. Nucl. Mater.* 392, 45-54.
- CERA, E., MERINO, J. & BRUNO, J. (2001): Release of radionuclides from spent fuel under repository conditions: mathematical modeling and preliminary results. *Mat. Res. Soc. Symp. Proc.* 663, 459-467.

- CHOI, H.W., MCEACHERN, R.J., TAYLOR, P. & WOOD, D.D. (1996): The effect of fission products on the rate of  $U_3O_8$  formation in SIMFUEL oxidized in air at 250°C. *J. Nucl. Mater.* 230, 250-258.
- CHRISTENSEN, H., SUNDER, S. & SHOESMITH, D.W. (1994): Oxidation of nuclear fuel  $UO_2$  by the products of water radiolysis: development of a kinetic model. *J. Alloys and Comps.* 213/214, 93-99.
- CHUMSENG, L., JINGRU, G. & DAMING, L. (1997): A procedure for the separation of  $^{79}Se$  from fission products and application to the determination of the  $^{79}Se$  half-life. *J. Radioanal. Nucl. Chem.* 220, 69-71.
- CLARENS, F., DE PABLO, J., DIAZ-PEREZ, I., CASAS, I., GIMENEZ, J. & ROVIRA, M. (2004): Formation of studtite during the oxidative dissolution of  $UO_2$  by hydrogen peroxide. *Environ. Sci. Technol.* 38, 6656-6661.
- COBOS, J., PAPAIOANNOU, D., SPINO, J. & COQUERELLE, M. (1998): Phase characterization of simulated high burn-up  $UO_2$  fuel. *J. Alloy Compd.* 271-273, 610-615.
- COBOS, J., HAVELA, I., RONDINELLA, V.V., DE PABLO, J., GOUDER, T., GLATZ, J.P., CARBOL, P. & MATZKE, H. (2002): Corrosion and dissolution studies of  $UO_2$  containing  $\alpha$ -emitters. *Radiochim. Acta* 90, 597-602.
- COBOS, J., WISS, T., GOUDER, T. & RONDINELLA, V.V. (2003): XPS and SEM studies on the corrosion of  $UO_2$  containing Pu in de-mineralized and carbonated water. *Mat. Res. Soc. Symp. Proc.* 757, 365-375.
- CRAMER, J.J. & J.A.T. SMELLIE. (1994): Final report of the AECL/SKB Cigar Lake analog study, Atomic Energy of Canada Limited Report, AECL-10851, COG-93-147, SKB TR 94-04.
- CUI, D. & SPAHIU, K. (2011): Environmental behaviour of spent nuclear fuel and canister materials. *Energy Environ. Sci.* 4, 2537-2545.
- CUI, D., SPAHIU, K. & WERSIN, P. (2003): Redox reactions of iron and uranium dioxide in simulated cement pore water under repository conditions. *Mat. Res. Soc. Symp. Proc.* 757, 427-433
- CUI, D., EKEROTH, E., FORS, P. & SPAHIU, K. (2008): Surface Mediated Processes in the Interaction of Spent Fuel or  $\alpha$ -doped  $UO_2$  with  $H_2$ . *Mat. Res. Soc. Symp. Proc.* 1104, 1104-NN03-05 doi:10.1557/PROC-1104-NN03-05.
- DE PABLO, J., CASAS, I., GIMENEZ, J., MARTI, V., & TORRERO, M.E. 1996. Solid surface evolution model to predict uranium release from unirradiated  $UO_2$  and nuclear spent fuel dissolution under oxidizing conditions. *J. Nucl. Mater.* 232, 138-145.
- DE PABLO, J., CASAS, I., JIMENEZ, J., MOLERA, M., ROVIRA, M., DURO, L. & BRUNO, J. (1999): The oxidative dissolution mechanism of uranium dioxide. The effect of temperature in hydrogen carbonate medium. *Geochim. Cosmochim. Acta* 63, 3097-3103.
- DE PABLO, J., CASAS, I., CLARENS, F., AAMRANI, EL. & ROVIRA, M. (2001): The effect of hydrogen peroxide concentration on the oxidative dissolution of unirradiated uranium dioxide. *Mat. Res. Soc. Symp. Proc.* 663, 409-426.
- DE PABLO, J., CASAS, I., GIMENEZ, J., CLARENS, F., DURO, L. & BRUNO, J. (2004): The oxidative dissolution mechanism of uranium dioxide. The effect of pH and oxygen partial pressure. *Mat. Res. Soc. Symp. Proc.* 807, 1-6.
- DE PABLO, J., SERRANO-PURROY, D., GONZALEZ-ROBLES, E., CLARENS, F., MARTINEZ-ESPARZA, A., WEGEN, D.H., CASAS, I., CHRISTIANSEN, B., GLATZ, J.-P. & GIMENEZ, J. (2009): Effect of HBS structure on the fast release fraction of 48 Gwd/tU PWR fuel. *Mat. Res. Soc. Symp. Proc.* 1193, 613-620.
- DESRANGES, L., BALDINOZZI, G., SIMON, P., GUIMBRETIERE, G. & CANIZARES, A. (2012): Raman spectrum of  $U_4O_9$ : a new interpretation of damage lines in  $UO_2$ . *J. Raman Spectrosc.* 43, 455-458.
- DIAZ-AROCAS, P., QUIÑONES, J., MAFFIOTTE, C., SERRANO, J., GARCIA, J., ALMAZAN, J.R. & ESTEBAN, J. (1995): Effect of secondary phase formation in the leaching of  $UO_2$  under simulated radiolytic products. *Mat. Res. Soc. Symp. Proc.* 353, 641-646.
- EKEROTH, E. & JONSSON, M. (2003): Oxidation of  $UO_2$  by radiolytic oxidants. *J. Nucl. Mater.* 322, 242-248.
- EKEROTH, E., ROTH, O. & JONSSON, M. (2006): The relative impact of radiolysis products in radiation induced oxidative dissolution of  $UO_2$ . *J. Nucl. Mater.* 355, 38-46.
- EKEROTH, E., LOW, J., ZWICKY, H-U. & SPAHIU, K. (2009): Corrosion studies with high burnup LWR fuel in simulated groundwater. *Mat. Res. Soc. Symp. Proc.* 1124, 123-128.

- ERIKSEN, T.E., EKLUND, U-B., WERME, L.O. & BRUNO, J. (1995): Dissolution of irradiated fuel: a radiolytic mass balance study. *J. Nucl. Mater.* 227, 76-82.
- ERIKSEN, T.E., SHOESMITH, D.W. & JONSSON, M. (2012): Radiation induced dissolution of UO<sub>2</sub> based nuclear fuel — A critical review of predictive modeling approaches. *J. Nucl. Mater.* 420, 409-423.
- FERRY, C., LOVERA, P., POINSSOT, E. & GARCIA, P. (2005): Enhanced diffusion under alpha self-irradiation in spent nuclear fuel: Theoretical approaches. *J. Nucl. Mater.* 346, 48-55.
- FERRY, C., POINSSOT, C., CAPPELAERE, C., DESGRANGES, L., JÉGOU, C., MISERQUE, F., PIRON, J.P., ROUDIL, D. & J.M. GRAS, J.M. (2006): Specific outcomes of the research on the spent fuel long-term evolution in interim dry storage and deep geological disposal. *J. Nucl. Mater.* 352, 246-253.
- FERRY, C., PIRON, J-P. & AMBARD, A. (2010): Effect of helium on the microstructure of spent fuel in a repository: An operational approach. *J. Nucl. Mater.* 407, 100-109.
- FINCH, R.J., BUCK, E.C., FINN, P.A. & BATES, J.K. (1999): Oxidative corrosion of spent UO<sub>2</sub> fuel in vapour and dripping groundwater at 90°C. *Mat. Res. Soc. Symp. Proc.* 556, 431-438.
- FINCH, R.J., FORTNER, J.A., BUCK, E.C. & WOLF, S.F. (2002): Neptunium incorporation into U(VI) compounds formed during aqueous corrosion of neptunium-bearing uranium oxide. *Mat. Res. Soc. Symp. Proc.* 713, 647-654.
- FINN, P.A., HOH, J.C., WOLF, S.F., SLATER, S.A. & BATES, J.K. (1996): The release of uranium, plutonium, cesium, strontium, technetium and iodine from spent fuel under saturated conditions. *Radiochim. Acta* 74, 65-71.
- FORBES, T.Z., HORAN, P., DEVINE, T., MCINNES, D. & BURNS, P. (2011): Alteration of dehydrated schoepite and soddyite to studtite, [(UO<sub>2</sub>) (O<sub>2</sub>) (H<sub>2</sub>O)<sub>2</sub>] (H<sub>2</sub>O)<sub>2</sub>. *Amer. Mineral.* 96, 202-206.
- FORS, P., CARBOL, P., VAN WINCKEL, S. & SPAHIU, K. (2009): Corrosion of high burn-up structured UO<sub>2</sub> fuel in the presence of dissolved H<sub>2</sub>. *J. Nucl. Mater.* 394, 1-8.
- GARISTO, F. (2002): Radionuclide and element specific data for the radionuclide screening model. Version 1.1. Ontario Power Generation Report No: 06819-REP-01200-10038-RO1.
- GIMENEZ, J., BARAJ, E., TORRERO, M.E., CASAS, I. & DE PABLO, J. (1996): Effect of H<sub>2</sub>O<sub>2</sub>, NaClO, and Fe on the dissolution of unirradiated UO<sub>2</sub> in 5 mol·kg<sup>-1</sup> NaCl. Comparison with spent fuel dissolution experiments. *J. Nucl. Mater.* 238, 64-69.
- GLATZ, J.-P., CARBOL, P., COBOS-SABATE, J., GOUDER, T., MISERQUE, F., GIMENEZ, J. & WEGEN, D. (2001): Release of radiotoxic elements from high burn-up UO<sub>2</sub> and MOX fuel in a repository. *Mat. Res. Soc. Symp. Proc.* 663, 449-458.
- GOLDIK, J.S., NOEL, J.J. & SHOESMITH, D.W. (2005): The electrochemical reduction of hydrogen peroxide on uranium dioxide electrodes in alkaline solution. *J. Electroanal. Chem.* 582, 241-248.
- GRAMBOW, B.G. & GIFFAUT, E. (2006): Coupling of chemical processes in the near field. *Mat. Res. Soc. Symp. Proc.* 932, 55-66.
- GRAMBOW, B., LOIDA, A., DRESSLER, P., GECKEIS, H., GAGO, J., CASAS, I., DE PABLO, J., GIMENEZ, J. & TORRERO, M.E. (1996): Long term safety of radioactive waste disposal: chemical reaction of fabricated and high burn-up spent fuel with saline brines. Wissenschaftliche Berichte, Forschungszentrum Karlsruhe FZKA 5702.
- GRAMBOW, B., LOIDA, A., MARTINEZ-ESPARZA, A., DIAZ-AROCAS, P., DE PABLO, J., MARX, G., GLATZ, J.P., LEMMENS, K., OLLILA, K. & CHRISTENSEN, H. (2000): Source term for performance assessment of spent fuel as a waste form, European Commission, Nuclear Science and Technology Report, EUR 19140 EN.
- GRAMBOW, B.G. *ET AL.* (2010): Model uncertainty for the mechanism of dissolution of spent fuel in nuclear waste repositories. Final Mikado Project report. European Commission, March 2010.
- GRANDSTAFF, D.E. (1976): A kinetic study of the dissolution of uraninite. *Econ. Geol. Bull. Soc. Econ. Geol.* 71, 1493-1506.
- GRAY, W.J., STRACHAN, D.M. & WILSON, C.N. (1991): Gap and Grain Boundary Inventories of Cs, Tc, Sr in Spent LWR Fuel. MRS 257.
- GRENTHE, I., FUGER, J., KONINGS, R.J., LEMIRE, R.J., MULLER, A.B., NGUYEN-TRUNG, C. & WANNER, H. (1992): Chemical Thermodynamics of Uranium, OECD Nuclear Energy Data Bank (Eds.), North Holland Elsevier Science, Amsterdam.

- GUILLAMONT, R., FANGHANEL, T., GRENTHE, I., NECK, V., PALMER, D. & RAND, M.H. (2003): Update on the chemical thermodynamics of uranium, neptunium, plutonium, americium and technetium, OECD-NEA, Chemical Thermodynamics Vol.5, 182-187, Elsevier, Amsterdam.
- HANSON, B.D. (1998): The burn-up dependence of light water reactor spent fuel oxidation, Pacific Northwest Laboratory Report, PNNL-11929, Richland, USA.
- HANSON, B., MCNAMARA, B., BUCK, E.C., FRUISE, J., JENSON, E., KRUPKA, K. & AIREY, B. (2005): Corrosion of spent nuclear fuel. 1. Formation of studtite and metastudtite. *Radiochim. Acta* 93, 159-168.
- HE, H. & SHOESMITH, D.W. (2010): Raman spectroscopic studies of defect structures and phase transitions in hyper-stoichiometric  $\text{UO}_{2+x}$ . *Phys. Chem. Phys.* 12, 8108-8117.
- HE, H., KEECH, P.G., BROCKOWSKI, M.E., NOEL, J.J. & SHOESMITH, D.W. (2007): Characterization of the influence of fission product doping on the anodic reactivity of uranium dioxide. *Can. J. Chem.* 85, 1-12.
- HE, H., DING, Z. & SHOESMITH, D.W. (2009): The determination of electrochemical reactivity and sustainability on individual hyper-stoichiometric  $\text{UO}_{2+x}$  grains by Raman microspectroscopy and scanning electrochemical microscopy. *Electrochem. Comm.* 11, 1724-1727.
- HE, H., BROCKOWSKI, M., O'NEIL, K., OFORI, D., SEMENIKHIN, O. & SHOESMITH, D.W. (2012): Corrosion of nuclear fuel ( $\text{UO}_2$ ) inside a failed nuclear waste container. Nuclear Waste Management Organization (Toronto), TR-2012-09.
- HOCKING, W.H., BETTERIDGE, J.S. & SHOESMITH, D.W. (1994): The cathodic reduction of oxygen on uranium dioxide in dilute alkaline aqueous solution. *J. Electroanal. Chem.* 379, 339-351.
- HOSSAIN, M.M. & JONSSON, M. (2008):  $\text{UO}_2$  oxidation site densities determined by one- and two- electron oxidants. *J. Nucl. Mater.* 373, 186-189.
- HOSSAIN, M.M., EKEROTH, E. & JONSSON, M. (2006): Effects of  $\text{HCO}_3^-$  on the kinetics of  $\text{UO}_2$  oxidation by  $\text{H}_2\text{O}_2$ . *J. Nucl. Mater.* 358, 202-208.
- HYLAND, G.J. & RALPH, J. (1983): Electronic contributions to the high temperature thermo-physical properties of  $\text{UO}_{2+}$ . A critical analysis. *High Temp. High Pressure* 15, 170-190.
- IAEA (2010): Review of Fuel Failure Rates in Water Cooled Reactors, IAEA Energy Series No. NF-T-2.1, IAEA Vienna.
- ICRP (International Commission in Radiological Protection) (1991): 1990 recommendation of the International Commission on Radiological Protection. *Annals of the ICRP* 21(1-3), ICRP Publication 60, Pergamon Press, Oxford.
- IGLESIAS, E. & QUIÑONES, J. (2008): Analogous materials for studying spent nuclear fuel: the influence of particle size distribution on the specific surface area of irradiated nuclear fuel. *Appl. Surf. Sci.* 254, 6890-6896.
- ILIN, S.R., SPAHIU, K. & EKLUND, U-B. (2001): Determination of dissolution rates of spent fuel in carbonate solutions under different redox conditions with a flow-through experiment. *J. Nucl. Mater.* 297, 231-243.
- JÉGOU, C., PEUGET, S., BROUDIC, V., RONDIL, D., DESCHANELS, X. & BART, J.M. (2004): Identification of the mechanism limiting the alteration of clad spent fuel segments in aerated carbonated groundwater. *J. Nucl. Mater.* 326, 144-155.
- JÉGOU, C., MUZEAU, B., BROUDIC, V., PEUGET, S., POLESQUEN, A., ROUDIL, D. & CORBEL, C. (2005): Effect of external gamma irradiation on dissolution of the spent  $\text{UO}_2$  fuel matrix. *J. Nucl. Mater.* 341, 62-82.
- JÉGOU, C., MUZEAU, B., BROUDIC, V., ROUDIL, D. & DESCHANELS, X. (2007): Spent fuel  $\text{UO}_2$  matrix alteration in aqueous media under oxidizing conditions. *Radiochim. Acta* 95, 513-522.
- JOHNSON, L.H. & MCGINNES, D.F. (2002): Partitioning of Radionuclides in Swiss Power Reactor Fuels: Swiss National Cooperative for the Disposal of radioactive Waste. Nagra Technical Report 02-07.
- JOHNSON, L.H. & SHOESMITH, D.W. (1988): Spent fuel. In: "Radioactive Wasteforms for the Future," edited by W.B. Lutze and R.C. Ewing. Elsevier Science Publishers B.V., Amsterdam, Netherlands, Chapter 11, 635-698.
- JOHNSON, L.H., LENEVEU, D.M., SHOESMITH, D.W., OSCARSON, D.W., GRAY, M.N., LEMIRE, R.J. & GARISTO, N.C. (1994): The disposal of Canada's nuclear fuel waste: The vault model for post closure assessment, Atomic Energy of Canada Ltd. Report AECL-10714, COG-94-4.

- JOHNSON, L.H., FERRY, C., POINSSOT, C. & P. LOVERA (2005): Spent fuel radionuclide source term model for assessing spent fuel performance in geological disposal. Part I: Assessment of the instant release fraction. *J. Nucl. Mater.* 346, 56-65.
- JONSSON, M., F. NIELSEN, F., ROTH, O., EKEROTH, E., NILSSON, S. & HOSSAIN, M.M. (2007): Radiation induced spent nuclear fuel dissolution under deep repository conditions. *Environ. Sci. Technol.* 41, 7087-7093.
- KEECH, P.G., GOLDIK, J.S., QIN, Z. & SHOESMITH, D.W. (2011): The anodic dissolution of SIMFUEL (UO<sub>2</sub>) in slightly alkaline sodium carbonate/bicarbonate solutions. *Electrochim. Acta* 56, 7923-7930.
- KING, F. & KOLAR, M. (2002): Validation of the mixed-potential model for used fuel dissolution against experimental data. Ontario Power Generation Report No: 06819-REP-01200-10077-R00.
- KING, F. & SHOESMITH, D.W. (2004): Electrochemical studies of the effect of H<sub>2</sub> on UO<sub>2</sub> dissolution. Swedish Nuclear Fuel and Waste Management Company Technical Report TR-04-20.
- KING, F. & SHOESMITH, D.W. (2010): Long term containment performance-corrosion behaviour of candidate canister materials, In: "Geological Repositories for Safe Disposal of Spent Nuclear Fuels and Radioactive Materials", edited by J. Ahn and M. Apted, Woodhead Publishing Ltd., Cambridge, U.K., Chapter 14.
- KING, F., QUINN, M.J. & MILLER, N.H. (1999): The effect of hydrogen and gamma radiation on the oxidation of UO<sub>2</sub> in 0.1 mol.L<sup>-1</sup> NaCl. Swedish Nuclear Fuel and Waste Management Company Report TR-99-27.
- KLEYKAMP, H. (1993): The solubility of selected fission products in UO<sub>2</sub> and PuO<sub>2</sub>. *J. Nucl. Mater.* 206, 82-86.
- KLEYKAMP, H. (1985): The chemical state of fission products in oxide fuels. *J. Nucl. Mater.* 131, 221-246.
- KLEYKAMP, H. (1988): The chemical state of fission products in oxide fuels at different stages of the nuclear fuel cycle. *Nuclear Technology* 80, 412-422.
- KLEYKAMP, H., PASCHOAL, J.O., PEJSA, R. & THUMMLER, F. (1985): Composition and structure of fission product precipitates in irradiated fuels: correlation with phase studies in the Mo-Ru-Rh-Pd and BaO-UO<sub>2</sub>-ZrO<sub>2</sub>-MoO<sub>3</sub> systems. *J. Nucl. Mater.* 130, 426-433.
- KUBATKO, K.-A., HELEAN, K.B., NAVROTSKY, A. & BURNS, P.C. 2003. Stability of Peroxide-Containing Uranyl Minerals. *Science* 302, 1191-1193.
- LEE, C.T., QIN, Z., ODZIEMKOWSKI, M. & SHOESMITH, D.W. (2005): The influence of groundwater anions on the impedance behaviour of carbon steel corroding under anoxic conditions. *Electrochim. Acta* 51, 1558-1568.
- LOIDA, A., GRANBOW, B. & GECKEIS, H. (1996): Anoxic corrosion of various high burn-up spent fuel samples. *J. Nucl. Mater.* 233, 11-22.
- LOIDA, A., GRAMBOW, B. & GECKEIS, H. (2001): Congruent and incongruent radionuclide release during matrix dissolution of partly oxidized high burn-up spent fuel. *Mat. Res. Soc. Symp. Proc.* 663, 417-426.
- LOIDA, A., GENS, R., METZ, V., LEMMENS, K., CACHOIR, C., MENNECART, T. & KIENZLER, B. (2009): CORROSION behaviour of high burn-up spent fuel in highly alkaline solutions. *Mat. Res. Soc. Symp. Proc.* 1193, 597-604.
- LOUSADA, C.M., TRUMMER, M. & JONSSON, M. (2012): Reactivity of H<sub>2</sub>O<sub>2</sub> towards different UO<sub>2</sub>-based materials: the relative impact of radiolysis products revisited. *J. Nucl. Mater.* In press.
- LUCUTA, P.G., VERRALL, R.A., MATZKE, H.-J. & PALMER, B.J.F. (1991): Microstructural features of SIMFUEL-simulated high burn-up UO<sub>2</sub>-based nuclear fuel. *J. Nucl. Mater.* 178, 48-60.
- MCEACHERN, R.J. & TAYLOR, P. (1998): A review of the oxidation of uranium dioxide at temperatures below 400°C. *J. Nucl. Mater.* 254, 87-121.
- MC MURRY, J., DIXON, D.A., GARRONI, J.D., IKEDA, B.M., STROES-GASCOYNE, S., BAUMGARTNER, P. & MELNYK, T.W. (2003): Evolution of a Canadian Deep Geologic Repository: Base scenario. Ontario Power Generation Report No: 06819-REP-01200-10092-R00.
- MUZEAU, B., JEGOU, C., DELAUNAY, F., BRODIC, V., BREVET, A., CATALETTE, H., SIMONI E. & CORBEL, C. (2009): Radiolytic oxidation of UO<sub>2</sub> pellets doped with alpha-emitters (<sup>238/239</sup>Pu). *J. Alloys and Comps.* 467, 578-589.

- NAAS, P., GARTENMANN, R., GOLSER, W., KUTSCHERA, M., SUTER, N.-A., SYNAL, M.J.M., WAGNER, E. WELD & WINTELER, G. (1996): A new half-life measurement of the long-lived fission product  $^{126}\text{Sn}$ . *Nucl. Instr. and Methods B* 114, 131-137.
- NECK, V. & KIM, J.I. (2001): Solubility and hydrolysis of tetravalent actinides. *Radiochim. Acta*. 89, 1-16.
- NICOL, M.J. & NEEDES, C.R.S. (1973): The mechanism of the anodic dissolution of uranium dioxide. Nat. Inst. Met. Repub. S. Africa, Report No.: 7079.
- NIELSEN, F. & JONSSON, M. (2006): Geometrical  $\alpha$ - and  $\beta$ - dose rate distributions and production rates of radiolysis products in water in contact with spent nuclear fuel. *J. Nucl. Mater.* 359, 1-7.
- NIELSEN, F. & JONSSON, M. (2007): On the catalytic effects of  $\text{UO}_2(\text{s})$  and  $\text{Pd}(\text{s})$  on the reaction between  $\text{H}_2\text{O}_2$  and  $\text{H}_2$  in aqueous solution. *J. Nucl. Mater.* 372, 160-163.
- NILSSON, S. & JONSSON, M. (2011):  $\text{H}_2\text{O}_2$  and radiation induced dissolution of  $\text{UO}_2$  and SIMFUEL pellets. *J. Nucl. Mater.* 410, 89-93.
- ODEGAARD-JENSEN, A. & OVERSBY, V. (2008): Testing of uranium dioxide containing different levels of alpha activity under anaerobic and reducing conditions. *Mat. Res. Soc. Symp. Proc.* 1104.
- OLLILA, K. (2007): Dissolution of unirradiated  $\text{UO}_2$  and  $\text{UO}_2$  doped with  $^{233}\text{U}$  in low and high ionic strength NaCl under anoxic and reducing conditions. European Commission NF-PRO Report D.1.5.11.
- OLLILA, K., ALBINSSON, Y., OVERSBY, V. & COWPER, M. (2003): Dissolution rates of unirradiated  $\text{UO}_2$ ,  $\text{UO}_2$  doped with  $^{233}\text{U}$ , and spent fuel under normal atmospheric conditions and under reducing conditions using on isotope dilution method. SKB Technical Report TR-03-13.
- OVERSBY, V.M. (1999): Uranium dioxide, SIMFUEL and spent fuel dissolution rates – A review of published data. Swedish Nuclear Fuel and Waste Management Company Technical report, TR-99-22.
- PAQUETTE, J. & LEMIRE, R.J. (1981): A description of the chemistry of aqueous solutions of uranium and plutonium to 200°C using potential—pH diagrams. *Nucl. Sci. Eng.* 79, 26-48.
- PASTINA, B. & LAVERNE, J.A. (2001): Effect of molecular hydrogen on hydrogen peroxide in water radiolysis. *J. Phys. Chem. A* 105, 9316-9322.
- PASTINA, B., ISABEY, J. & HICKEL, B. (1999): The influence of water chemistry on the radiolysis of primary coolant water in pressurized water reaction. *J. Nucl. Mater.* 264, 309-318.
- PEHRMAN, R., TRUMMER, M., LOUSADA, C. & JONSSON, M. (2012): On the redox reactivity of doped  $\text{UO}_2$  pellets-influence of dopants on the  $\text{H}_2\text{O}_2$  decomposition mechanism. *J. Nucl. Mater.* 430, 6-11.
- POINSSOT, C., JÉGOU, C., TOULHOAT, P., PIRON, J.-P. & GRAS, J.-M. (2001): A new approach to the RN source term for spent nuclear under geological disposal conditions. *Mat. Res. Soc. Symp. Proc.* 663, 469-476.
- POINSSOT, C., FERRY, C., KELM, M., GRAMBOW, B., MARTINEZ-ESPARZA, A., JOHNSON, L., ANDRIAMBOLOLONA, Z., BRUNO, J., CACHOIR, C., CAVENDON, J.-M., CHRISTENSEN, H., CORBEL, C., JÉGOU, C., LEMMENS, K., LOIDA, A., LOVERA, P., MISERQUE, F., DE PABLO, J., POULESQUEN, A., QUIÑONES, J., RONDINELLA, V., SPAHIU, K. & WEGEN, D. (2005): Final report of the European project spent fuel stability under repository conditions. European Commission Report CEA-R-6093.
- QUIÑONES, J., SERANO, J.A., DIAZ AROCAS, P., RODRIGUEZ-ALMEZAN, J.L., COBOS, J., ESTEBAN, J.A. & MARTINEZ-ESPARZA, A. (2001): Influence of container base material (Fe) on SIMFUEL leaching behavior. *Mat. Res. Soc. Symp. Proc.* 663, 435-439.
- RAMEBACK, H., ALBINSSON, Y., SKALBERY, M. & WERME, L. (1994): Release and diffusion of  $^{90}\text{Sr}$  from spent  $\text{UO}_2$  fuel in bentonite clay. *Radiochim. Acta* 66/67, 405-408.
- ROLLIN, S., SPAHIU, K. & EKLUND, U.-B. (2001): Determination of dissolution rates of spent fuel in carbonate solutions under different redox conditions with a flow through experiment. *J. Nucl. Mater.* 297, 231-243.
- RONDINELLA, V.V. & T. WISS, T. (2010): The High Burn-up Structure in Nuclear Fuel; *Materials Today* 13(12) 24-32.
- RONDINELLA, V.V., MATZKE, H.J., COBOS, H. & WISS, T. (1999): Leaching behaviour of  $\text{UO}_2$  containing  $\alpha$ -emitting actinides. *Radiochim. Acta* 88, 1-5.

- ROTH, O & JONSSON, M. (2009): On the impact of reactive solutes on radiation induced oxidative dissolution of  $\text{UO}_2$ . *J. Nucl. Mater.* 385, 595-600.
- ROUDIL, D., JÉGOU, C., BROUDIC, V., MUZEAU, B., PEUGET, S. & DESCHANELS, X. (2007): Gap and grain boundary inventories from pressurized water reactor spent fuel. *J. Nucl. Mater.* 362, 411-415.
- ROUDIL, D., JÉGOU, C., BROUDIC, V. & TRIBET, M. (2009): Rim Instant release radionuclide inventory from French burnup spent MOX fuel. *Mat. Res. Soc. Symp. Proc.* 1193, 627-633.
- SALAH, S., CACHOIR, C., LEMMENS, K. & MAES, N. (2006): Static dissolution tests of alpha-doped  $\text{UO}_2$  under repository relevant conditions: Influence of Boom Clay and alpha activity on fuel dissolution rates. *Mat. Res. Soc. Symp. Proc.* 932, 481-488.
- SANTOS, B.G., NESBITT, H.W., NOEL, J.J. & SHOESMITH, D.W. (2004): X-ray photoelectron spectroscopy study of anodically oxidized SIMFUEL surfaces. *Electrochim. Acta* 49, 1863-1873.
- SANTOS, B.G., NOEL, J.J. & SHOESMITH, D.W. (2006): The influence of calcium ions on the development of acidity in corrosion product deposits on SIMFUEL ( $\text{UO}_2$ ). *J. Nucl. Mater.* 350, 320-331.
- SATTONAY, G., ARDOIS, C., CORBEL, C., LUCCHINI, J.F., BARTHE, M.-F., GARRIDO, F. & GORSET, D. (2001): Alpha-radiolysis effects on  $\text{UO}_2$  alteration in water. *J. Nucl. Mater.* 288, 11-19.
- SHOESMITH, D.W. (2000): Fuel corrosion processes under waste management conditions. *J. Nucl. Mater.* 282, 1-31.
- SHOESMITH, D.W. (2007): Used fuel and uranium dioxide dissolution studies — A review, Nuclear Waste Management Organization (Toronto) Report TR-2007-03.
- SHOESMITH, D.W. (2007): Used fuel and uranium dioxide dissolution studies – A review. Nuclear Waste Management Technical Report NWMO TR-2007-03. Toronto, Canada.
- SHOESMITH, D.W. & SUNDER, S. (1991): An electrochemistry-based model for the dissolution of  $\text{UO}_2$ , Atomic Energy of Canada Report, AECL-10488.
- SHOESMITH, D.W. & SUNDER, S. (1992): The prediction of nuclear fuel ( $\text{UO}_2$ ) dissolution rates under waste disposal conditions. *J. Nucl. Mater.* 190, 20-35.
- SHOESMITH, D.W., SUNDER, S. & HOCKING, W.H. (1994): Electrochemistry of  $\text{UO}_2$  nuclear fuel. In: “Electrochemistry of Novel Materials”, edited by J. Lipkowski and P.N. Ross, VCH Publishers, New York, Chapter 6, 297-337.
- SHOESMITH, D.W., SUNDER, S. & TAIT, J.C. (1998): Validation of an electrochemical model for the oxidative dissolution of used CANDU fuel. *J. Nucl. Mater.* 257, 89-98.
- SHOESMITH, D.W., SUNDER, S. & BETTERIDGE, J.S. (2000): The influence of alpha-radiolysis on  $\text{UO}_2$  fuel dissolution as observed in electrochemical experiments. Ontario Power Generation Report No.: 06819-REP-01200-10047-1200.
- SHOESMITH, D.W., KOLAR, M. & KING, F. (2003): A mixed potential model to predict fuel (uranium dioxide) corrosion within a failed nuclear waste container. *Corrosion* 59, 802-816.
- SHOESMITH, D.W., NOEL, J.J., QIN, Z., LEE, C.T., SANTOS, B.G. & BROCKOWSKI, M.E. (2004): Corrosion of nuclear fuel inside a failed waste container. Ontario Power Generation Report No.: 06819-REP-01200-10145-R00.
- SKB (2010): Fuel and Canister Process Report for the Safety Assessment SR-site. Swedish Nuclear Fuel and Waste Management Company Technical Report TR-10-46.
- SMART, N.R., BLACKWOOD, D.J. & WERME, L.O. (2002a): Anaerobic corrosion of carbon steel and cast iron in artificial groundwater. Part I — electrochemical aspects. *Corrosion*. 58, 547-559.
- SMART, N.R., BLACKWOOD, D.J. & WERME, L.O. (2002b): Anaerobic corrosion of carbon steel and cast iron in artificial groundwater. Part II – Gas generation. *Corrosion*. 58, 627-637.
- SPAHIU, K., CIU, D. & LUNDSTROM, M. (2004): The fate of radiolytic oxidants during spent fuel leaching in the presence of dissolved near field hydrogen. *Radiochim. Acta* 92, 625-629.
- SPAHIU, K., EKLUND, U.-B., CIU, D. & LUNDSTROM, M. (2002): The influence of nene filled redox conditions on spent fuel leaching. *Mat. Res. Soc. Symp. Proc.* 713, 633-638.
- STROES-GASCOYNE, S. (1996): Measurements of instant-release source terms for  $^{137}\text{Cs}$ ,  $^{90}\text{Sr}$ ,  $^{99}\text{Tc}$ ,  $^{129}\text{I}$  and  $^{14}\text{C}$  in used CANDU fuel. *J. Nucl. Mater.* 238, 264-277.
- STROES-GASCOYNE, S., JOHNSON, L.H. & SELLINGER, D.M. (1987): The relationship

- between gap inventories of stable xenon and  $^{137}\text{Cs}$  and  $^{129}\text{I}$  in used fuel. *Nucl. Tech.* 77, 320-330.
- STROES-GASCOYNE, S., JOHNSON, L.H., SELLINGER, D.M. & WILKIN, D.L. (1992a): Release of fission products and actinides from used CANDU fuel fragments under reducing conditions at 100°C. Atomic Energy of Canada Ltd. Report, AECL-10574, COG-92-31.
- STROES-GASCOYNE, S., TAIT, J.C., GARISTO, N.C., PORTH, R.J., ROSS, J.P.M., GLOWA, G.A. & BARNDALE, T.R. (1992b): Instant release of  $^{14}\text{C}$ ,  $^{99}\text{Tc}$ ,  $^{90}\text{Sr}$ , and  $^{137}\text{Cs}$  from used CANDU fuel at 25°C in distilled deionized water. *Mat. Res. Soc. Symp. Proc.* 257, 373-380.
- STROES-GASCOYNE, S., MOIR, D.L., KOLAR, M., PORTH, R.J., MCCONNELL, J.L. & KERR, A.N. (1994): Measurement of Gap and Grain Boundary Inventories of  $^{129}\text{I}$  used in CANDU fails. *Mat. Res. Soc. Symp.* 353.
- STROES-GASCOYNE, S., KING, F., BOTTERIDGE, J.S. & GARISTO, F. (2002): The effects of alpha-radiolysis on  $\text{UO}_2$  dissolution determined from electrochemical experiments with  $^{238}\text{Pu}$ -doped  $\text{UO}_2$ . *Radiochim. Acta* 90, 603-609.
- STUMM, W. (editor) (1990): *Aquatic chemical kinetics. Reaction rates of processes in natural waters.* John Wiley, New York, NY.
- SUNDER, S., BOYER, G.D. & MILLER, N.H. (1990): XPS studies of  $\text{UO}_2$  oxidation by alpha radiolysis of water at 100°C. *J. Nucl. Mater.* 175, 163.
- SUNDER, S., SHOESMITH, D.W., CHRISTENSEN, H. & MILLER, N.H. (1992): Oxidation of  $\text{UO}_2$  fuel by the products of the gamma radiolysis of water. *J. Nucl. Mater.* 190, 781.
- SUNDER, S., SHOESMITH, D.W. & MILLER, N.H. (1997): Oxidation and dissolution of nuclear fuel ( $\text{UO}_2$ ) by the products of the alpha radiolysis of water. *J. Nucl. Mater.* 244, 66-74.
- SUNDER, S., MILLER, N.H. & SHOESMITH, D.W. (2004): Corrosion of uranium dioxide in hydrogen peroxide solutions. *Corr. Sci.* 46, 1095-1111.
- SUTTON, H.C. & WINTERBOURN, C.C. (1989): On the participation of higher oxidation states of iron and copper in Fenton reactions. *Free Rad. Biol. Med.* 6, 53-60.
- TAIT, J.C., STROES-GASCOYNE, S., HOCKING, W.H., DUCLOS, A.M., PORTH, R.J. & WILKIN, D.L. (1991): Dissolution behaviour of used CANDU fuel under disposal conditions. *Mat. Res. Soc. Symp. Proc.* 212, 189-196.
- TAIT, J.C., ROMAN, H. & MORRISON, C.A. (2000): Characteristics and radionuclides inventories of used fuel from OPG Nuclear Generating Stations. Ontario Power Generation Report Volume 1 — Min Report 06819-REP-01200-10029-1200.
- THOMAS, L.E., EINZIGER, R.E. & BUCHANAN, H.C. (1993): Effect of fission products on air-oxidation of LWR spent fuel. *J. Nucl. Mater.* 201, 310-319.
- WINTER, P.W. (1989): The electronic transport properties of  $\text{UO}_2$ . *J. Nucl. Mater.* 161, 38-43.
- WREN, J.C., SHOESMITH, D.W. & SUNDER, S. (2005): Corrosion behaviour of uranium dioxide in alpha radiolytically decomposed water. *J. Electrochem. Soc.* 152, B470-B481.
- WRONKIEWICZ, D.J. (1999): Uranium: Mineralogy, Geochemistry and the Environment, Reviews in Mineralogy and Geochemistry, Mineralogical Society of America, Washington, D.C. 38, 475.
- WRONKIEWICZ, D.J., BATES, J.K., WOLF, S.F. & BUCK, E.C. (1996): Ten year results from unsaturated drip tests with  $\text{UO}_2$  at 90°C: Implications for the corrosion of spent nuclear fuel. *J. Nucl. Mater.* 238, 78-95.
- WU, L., BEANREGARD, Y., QIN, Z., ROHANI, S. & SHOESMITH, D.W. (2012): A model for the influence of steel corrosion products on nuclear fuel corrosion under permanent disposal conditions. *Corrs. Sci.* 61, 83-91.